

Chapter 1

Cardiac Remodeling and Molecular Mechanisms in Heart Failure

Hiroshi Okamoto, M.D., and Akira Kitabatake, M.D.

Introduction

The term “heart failure” is used to describe the pathophysiological state in which an abnormality of cardiac function is responsible for failure of the heart to pump blood at a rate commensurate with the requirements of the metabolizing tissues¹⁾. Cardiac function can be viewed as functional responses that develop rapidly. These responses are affected by mechanisms like altered calcium fluxes and posttranslational phosphorylation.

Recently, it has been demonstrated that heart failure is characterized by elevated concentrations of neurohumoral mediators such as angiotensin II and norepinephrine. There is a cross talk between the adrenergic system and renin-angiotensin system, both of which alter calcium fluxes and show maladaptive persistent activation in chronic heart failure. Blockade of both systems could prolong the life expectancy in heart failure. Heart failure is a systemic disease state. We tried to reveal that extracellular stimuli are detected by target cells through plasma membrane receptors by using a cardiomyopathic hamster as an in-vivo model of heart failure. Signal transduction constitutes a vital part in the interaction between cells in organs. Multiple alterations in alpha and beta-receptor signal transduction have been described in the failing remodeled myocardium^{2), 3)}. Neurohumoral mediators including norepinephrine and angiotensin II transmit their signals through signal transduction proteins such as Gq and Gs to activate a family of enzymes such as PKC and MAPK that induce the fetal gene program. Changes in beta-receptor signal transduction were viewed as partially adaptive changes, serving the useful purpose of withdrawing the cardiac myocytes from harmful adrenergic stimulation. These altered signaling systems might be responsible for the progression of myocardial function and remodeling.

The essential functions of the heart are performed at the level of the microvasculature, where oxygen, nutrients and hormones are delivered and catabolites are removed. The function of microvasculature depends on its diameter. Capillary vessels less than 30 μ m could contribute to the oxygen and energy transportation, and the regulation of vascular permeability. Abnormalities of the microvasculature such as reductions in capillary density, thickening of the walls of arterioles, inadequate angiogenesis are involved in the pathogenesis of various forms of heart disease^{4), 5)}. Myocardial neovascularization is an important physiological process that frequently occurs in chronic myocardial ischemia. In an acute phase of ischemia, irreversible myocyte necrosis might cause failure of angiogenesis to compensate. In fact, a significant collateralization has been demonstrated

together with reduction in the size of the infarct after intracoronary administration of growth factor in rabbits. The formation of capillaries could be demonstrated by injection of recombinant acidic fibroblast growth factor (aFGF) in patients with three-vessel coronary disease⁶. Cardiac remodeling is involved in cardiac hypertrophy, fibroblast proliferation, and extracellular matrix production leading to the progress of heart failure. Interstitial fibrosis may increase the diffusion distances from capillaries to myocytes. Coronary endothelial dysfunction has been demonstrated in heart failure and dilated cardiomyopathy (DCM)⁷. Thus, cardiac remodeling may result in abnormalities of the microvasculature and impaired angiogenesis after myocyte loss could participate in the process of cardiac remodeling. However, abnormalities in microvasculature and neovascular formation in the process of cardiac remodeling and the relationship between angiogenesis and cardiac remodeling have not been elucidated in DCM and heart failure. We hypothesized that alterations in microcirculation, especially in capillary microvasculature might be related to the progress of remodeling process. Accordingly, the goals of the present study were (1) to clarify the relationship between the progress in cardiac remodeling and alterations in capillary microvasculature leading to progressive deterioration in cardiac function and (2) to investigate the effect of pharmacological treatment on the capillary microvasculature and cardiac angiogenesis in dilated cardiomyopathy.

In addition to neurohumoral activation such as rennin-angiotensin system and sympathetic nerve system, a number of pro-inflammatory cytokines are activated in heart failure. In some pathophysiological conditions such as myocarditis, DCM, T cell activation is supposed to be responsible for myocardial injury. Interactions of T-cell surface receptors CD28 and CD40L with their ligands B7 and CD40, respectively, on antigen presenting cells (APCs) are critical for antigen-specific T cell activation under physiological and pathological conditions⁸. To achieve effective inhibition of these interactions, we constructed an adenovirus vector, AdexCTLA4IgG, containing the extracellular domain of murine CTLA4 and the Fc portion of a human immunoglobulin G1, then examined the effects of these adenovirus vectors in the treatment of failing heart. CTLA4Ig blocks specifically the costimulatory signal between APCs and T cells only when antigen was presented. Moreover, AdexCTLA4Ig causes persistent and efficient expression *in vivo* for a long period and termination at the desired time, but has not been clinically evaluated⁹. ICOS is on the same line of CTLA4, but the mechanism responsible for its activation is somewhat different from that for CTLA4⁹. Anyway, our study indicates the therapeutic potential of the gene-transfer method in myocarditis, cardiac transplantation and ischemia-reperfusion injury after cardiac transplantation. DCM and other T-cell-mediated autoimmune heart diseases may be on the same line. However, therapeutic strategies might be influenced by the underlying disease, etiology, stage and extent of its attribution as shown by the former studies. In addition, blockade of T cell costimulatory signals might be an efficient and

helpful tool to eliminate graft rejection and graft versus host disease in cardiac transplantation and cell transplantation, in which autoimmunity could be induced¹⁰. Prolongation of other gene expressions using various types of virus vectors may be relevant in human gene therapy. To develop more specific immunomodulating agents for the treatment of heart failure, further research may be needed to precisely identify the most important players.

Very limited epidemiological data are available regarding the prognosis of heart failure and temporal changes in survival in a population-based setting in Japan. It is estimated from the total sales of digitalis, its prescription rate and usage ratio for arrhythmias that at least one million of patients suffer from heart failure in Japan. Dilated cardiomyopathy (DCM) is a major cause of severe heart failure. Over the past 27 years, three cohorts corresponding to three different periods of 9 years were investigated. Ten-year survivals were progressively improved. Patients were older and less severely affected, partly explaining the improvement in survival. In the subgroups treated with ACE inhibitors and beta blockers, calculated ten-year survival rate reached over 90%.

As the Human Genome Project moves toward completion, research efforts to identify genes related to heart failure will move forward at a more rapid pace. The underlying mechanisms for heart failure will be determined by not only genetic information, but also by integrated method to clarify the structure and function of molecules. System is consisted of many components. In post-genome era, it is necessary to understand a whole system through reconstruction of its components.

1. Renin-angiotensin System in Heart Failure

Nowadays, spontaneously hypertensive rats (SHR) are widely used as a low renin model of human essential hypertension. However, little is known about the regulation of cardiac RAS gene expression in hypertrophied hearts of SHR. As shown in the upper panel of figure1, systolic blood pressure, left ventricular to body weight ratio and cardiac ACE activity showed no significant difference between SHR and normotensive WKY rats at the age of 5 weeks, and those measurements were increased at the age of 10 weeks in SHR, but not in WKY. As shown in the lower panels of figure1, mRNA expression for angiotensinogen, renin and ACE was enhanced about 2-fold in left ventricles of SHR compared with WKY at the age of 10 weeks. Ten-week-old SHR were treated with hydralazine or thiazide for 4 weeks and compared with untreated SHR. In the groups treated with either thiazide or hydralazine, systolic blood pressure decreased. However, the left ventricular to body weight ratio remained unchanged in the hydralazine group. In each treated group, mRNA expression of ACE and ACE activity decreased compared with untreated SHR. In SHR treated with thiazide, plasma renin activity increased compared with the untreated and hydralazine-treated groups. These findings suggest that elevation of blood pressure is a primary factor for cardiac RAS activation, which may cause LV hypertrophy, but that suppression of cardiac

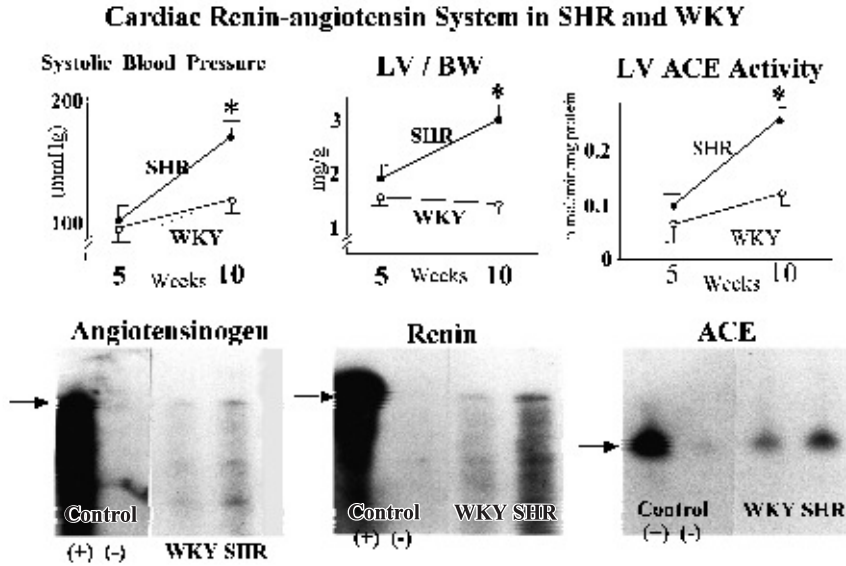


Figure 1 Upper Panel from left to right: systolic blood pressure (mmHg), left ventricular weight and left ventricular ACE activity (nmol/min/mg protein) of SHR and WKY at the ages of 5 weeks and 10 weeks. Lower Panel from left to right: mRNA expressions for angiotensinogen, renin and ACE of SHR and WKY at the ages of 5 weeks and 10 weeks by ribonuclease protection assay.

RAS does not always cause regression of LV hypertrophy. In LV hypertrophy, extracellular matrix protein, fibrillar collagen as well as myocytes are major components of the LV wall^{11), 12)}. We examined the effect of angiotensin II on collagen synthesis in cultured cardiac fibroblasts isolated from left ventricles of 10-week-old SHR and WKY. Twenty-four-hour stimulation of cardiac fibroblasts with angiotensin II resulted in an over 2-fold increase in collagen synthesis, which was completely inhibited by an angiotensin II type 1 antagonist, MK954 (figure 2). Cardiac RAS activation may cause myocardial fibrosis by stimulating collagen synthesis¹³⁾⁻¹⁶⁾.

2. Renin-angiotensin System and Cardiac Remodeling Process in Heart Failure Introduction

As myocardial remodeling is a central feature in the progression of myocardial failure, suppression of the activation of angiotensin II is important. In addition to reducing angiotensin II production, ACE inhibitors can influence other enzyme systems and bioactive peptide levels such as bradykinin, neurotensin, and substance P. Bradykinin induces to production of nitric oxide and prostaglandin in myocardium and these peptides play a role in reducing of cardiac remodeling. On the other hand, as AT₂ receptor may be reexpressed in heart failure, AT₂ antagonism, induced by AT₁ receptor blocker, may inhibit cell growth and fibrillar col-

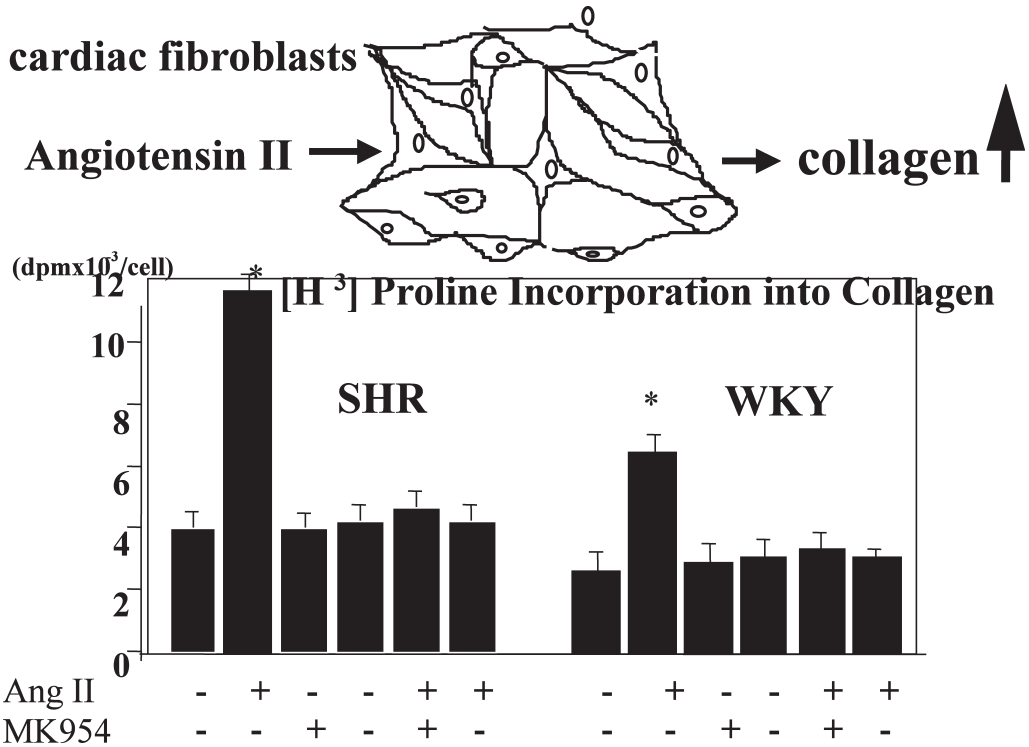


Figure 2 The effect of angiotensin II on collagen synthesis in cultured cardiac fibroblasts isolated from left ventricles of 10-week-old SHR and WKY. Twenty-four-hour stimulation of cardiac fibroblasts with (+) or without (-) angiotensin II (+) concomitantly with (+) or without (-) an angiotensin II type 1 antagonist, MK954.

Results are shown as mean values of dpm×10³/cell±SEM by [H³] Proline Incorporation into Collagen. *p<0.05, compared with fibroblasts without any stimulation. (from Ref. 17)

lagen metabolism. Moreover, chymase, a serine ptotease, is likely to play an important role in cardiac angiotensin II formation, because it is responsible for majority of angiotensin II production in human heart, so AT1 receptor antagonists can block the effects through the AT1 receptor agonism more effectively than ACE inhibitor. Although some studies have reported the different effects between ACE inhibitors and AT1 receptor blocker in the treatment heart failure, there are a few reports which have compared their different mechanism. Combined therapy with an ACE inhibitor and AT1 receptor antagonist results in more complete suppression of the renin-angiotensin system. Their combination therapy may provide unique effects in the setting of CHF by enhancing the effects of ACE inhibitor as well as preventing AT1 receptor activation from alternative Ang II-forming pathway of ACE inhibitors. However, there is little information about the effect of combined therapy in cardiac remodeling of cardiomyopathy¹⁷⁾.

In this study, using DCM hamsters, we examined that the comparable effects of

treatment of ACE inhibitor alone, AT1 receptor antagonist alone, and either ACE inhibitor and AT1 receptor antagonist, on cardiac function, cardiac remodeling and coronary microvasculature.

Materials and Methods

Experimental animals

The investigation conformed with the Guide for the Care and Use of Laboratory Animals published by the US National Institutes of Health (NIH Publication No. 85-23, revised 1985). All experiments were carried out using male TO2 cardiomyopathic hamsters (Bio Breeders Inc., Fitchburg, USA) and age-, sex-matched F1b hamsters were used as controls.

Echocardiography

The method was described previously¹⁸⁾. Briefly, each hamster was anesthetized with intraperitoneal injection of urethane (0.5mg/body mass) and α -chloralose (100mg/kg) and transthoracic echocardiograms (Hitachi EUB 565A) were obtained with a 7.5 MHz sector scanner. M-mode echocardiograms were recorded and the left ventricular end-diastolic dimension (LVDD) and percent fractional shortening (%FS) were determined. Pulsed-wave Doppler echocardiograms of mitral flow velocity obtained with the transducer at the cardiac apex were recorded, and isovolumic relaxation time (IRT) was measured.

Hemodynamic study

Each hamster was anesthetized with intraperitoneal injection of urethane (0.5 mg/body mass) and α -chloralose (100 mg/kg), and then artificially ventilated with oxygen-enriched air supplied by a Harvard respiratory system (tidal volume 1.2ml, respiration rate 100 cycle/min). After thoracotomy with care taken to minimize the volume of bleeding, a 2-French microtip catheter manometer (SPC-320, Millar Instruments, Inc., Houston, USA) with a TCB-500 control unit (Millar Instruments, Inc., Houston, USA) was inserted through the left ventricular apex using a 22 gauge needle for puncture. As indices of hemodynamics, the maximum rate of rise of ventricular pressure (dP/dTmax), the peak rate of pressure fall of ventricular pressure (dP/dTmin), the rate of the maximum velocity of shortening of unloaded contractile elements (Vmax) and the time constant of the exponential fit of the time course of isovolumic pressure decline (Tau) were obtained from left ventricular pressure by analysis with a computer system (MP-100WS, BIOPAC System, Inc., Santa Barbara USA) and the Acknowledge 2.0 program for the Macintosh (BIOPAC System, Inc., Santa Barbara USA).

To examine the temporal process of cardiac remodeling, we used cardiomyopathic hamsters, BIO TO2. The upper two panels of figure 3. show representative cross sectional views obtained from control F1b and BIO hamsters at the age of 26 weeks. In BIO, the ventricular wall is obviously thinner and left ventricle is more dilated than in F1b. And interstitial fibrosis is distinguished in BIO. Microscopic findings in the lower panels of Color fig. 1 show hypertrophied

myocytes and increased interstitial space in BIO. The numerical nuclear density was calculated by morphometrical analysis, which is shown in the left panel of figure 3. At the age of 5 weeks, there was no difference between BIO and F1b, but the numerical nuclear density was more decreased at the ages of 13 and 20 weeks in BIO. The numerical nuclear density is well correlated with percent fractional shortening as shown in the right panel of figure 3. While total collagen content remained unchanged with age in F1b, but it increased with age in BIO and showed significant differences at the ages of 10 to 20 weeks as shown in the left panel of figure 4. Total collagen content had a good correlation with percent fractional shortening as shown in the right panel of figure 4. These findings indicated that an increase in collagen content may lead to LV dysfunction. The left upper panel of figure 5 shows a cartoon of the angiotensin II signaling system modified from Dr. Opie. In normal circumstances, angiotensin II signaling can be mediated by Gq coupling PI-specific PLC, and the resultant production of DG and IP₃ causes an increase in intracellular Ca concentration and activate PKC.

PKC plays a role in cellular hypertrophy and damage in the reperfusion period. We demonstrated that the activities of ACE and PI-specific PLC were enhanced in

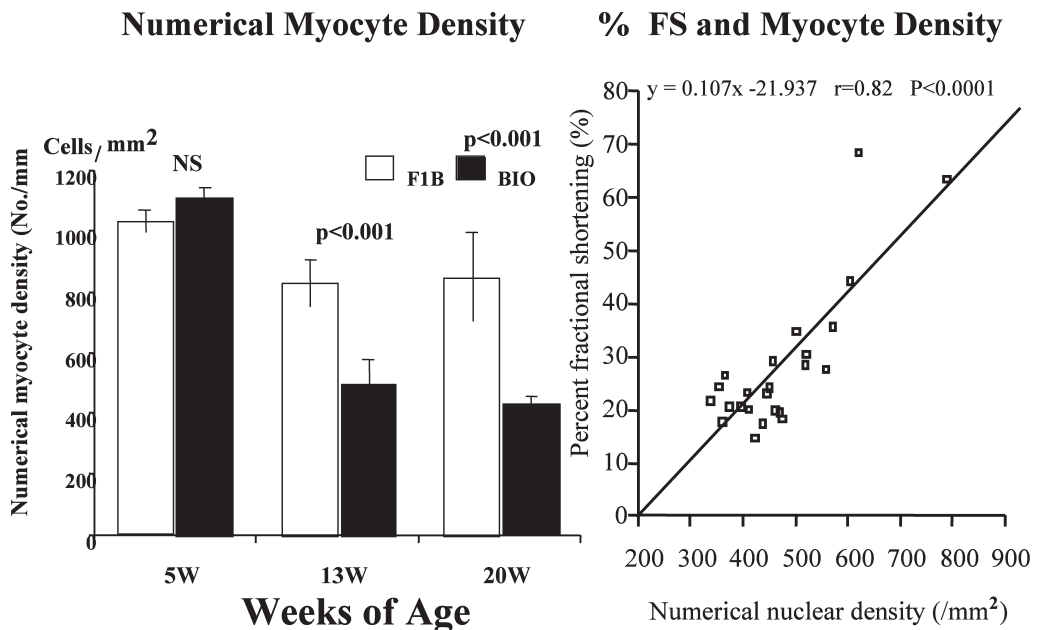


Figure 3 Left Panel: Numerical myocyte density (myocyte cell numbers per square millimeter) at the ages of 5, 13 and 20 weeks in TO2 and F1b strains of hamsters. Black bars show those of BIO and white bars F1b. Results are shown as mean \pm SEM from individual preparations. $p < 0.001$, compared with myocyte density of F1b hamsters. NS: non significant. Right Panel: The relationship between percent fractional shortening (%FS) and numerical myocyte density. Coefficient curve shows that $y = 0.107 \times 21.937$ $r = 0.82$, $P < 0.0001$.

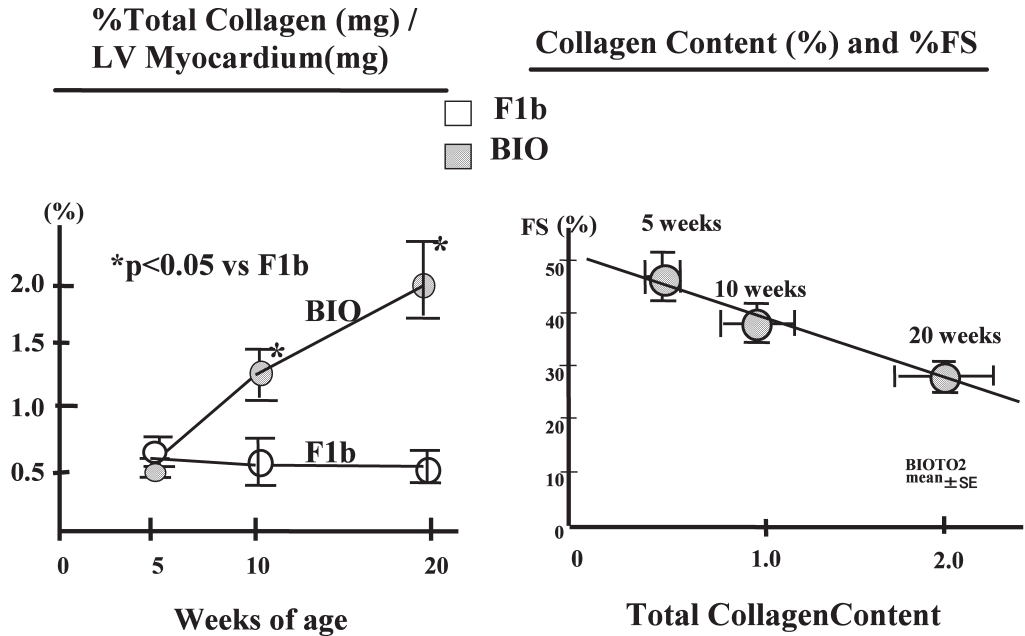


Figure 4 Left Panel: Percent ratios of the total collagen contents to left ventricular myocardium weight at the ages of 5, 10 and 20 weeks in TO2 (●) and F1b (○) strains of hamsters. Results shown are mean±SEM from individual preparations. $p < 0.05$, compared with myocyte density of F1b hamsters. Right Panel: The relationship between percent fractional shortening (%FS) and percent collagen content.

BIO in comparison to control F1b hamsters. Their activation may cause increases in IP3 and DG production in BIO. In fact, IP3 release was markedly enhanced by angiotensin II in BIO as shown in the right upper panel of figure 5 and the intracellular calcium concentration was higher in BIO at 5 to 20 weeks of age. These findings suggest that angiotensin II formation via ACE is enhanced and with angiotensin II signaling, PI turnover produces a higher intracellular calcium level in BIO. Thus, enhanced cardiac RAS may contribute to progress in cardiac remodeling process in this model.

In the remodeling process, myocyte apoptosis is known to be involved. We examined whether cardiac apoptosis could contribute to ACE mediated remodeling. Since hemodynamic overload activates neurohumoral factors other than cardiac RAS, we developed an in-vivo system, in which the human ACE gene could be transfected using an adenovirus vector. The heart was removed from the donor Wistar rat and the human ACE or LacZ gene was transfected, then the heart was transplanted into the abdominal aorta and inferior vena cava of another rat (Color fig. 2). To confirm the efficiency of this method, X-gal staining was performed and showed that about 30% of myocyte were positively stained 3 weeks after heart transplantation as shown in the lower left panel of Color fig. 2. Nested PCR

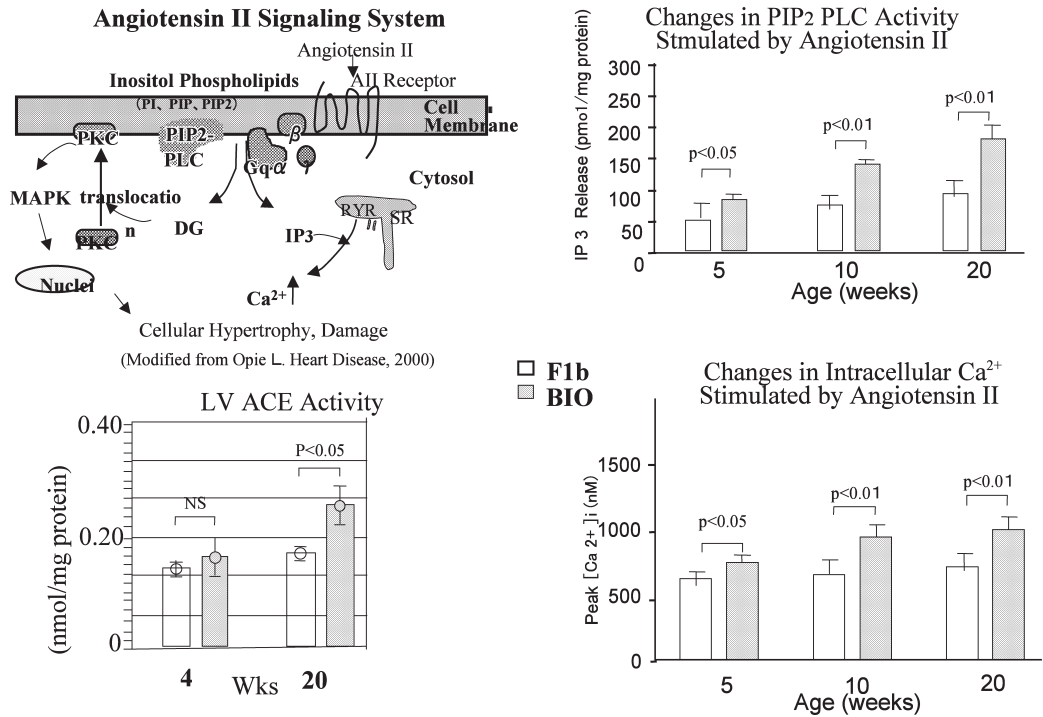


Figure 5 The left Upper Panel: Schematic drawing of the angiotensin II signaling system modified from Dr. Opie. In normal circumstances, angiotensin II signaling can be mediated by Gq coupling Phosphatidylinositol (PI)-specific phospholipase C (PLC), and the resultant production of diacylglycerol (DG) and inositol triphosphate (IP₃) causes an increase in intracellular Ca concentration and activate protein kinase C (PKC). PKC plays a role in cellular hypertrophy and damage in the reperfusion period. Left Lower Panel: Left ventricular ACE activity in LV expressed by nmol/mg protein at the ages of 4 and 20 weeks. Right Upper Panel: Changes in PIP₂ specific PLC activities at 5, 10 and 20 weeks of age. Results are shown as mean values of IP₃ Release (pmol/mg protein) ± SEM. Right Lower Panel: Changes in Intracellular Ca²⁺ Stimulated by Angiotensin II at the ages of 5, 10 and 20 weeks. Results are shown as mean values of Peak [Ca²⁺]_i (nM) ± SEM. (from Ref. 283)

detected a human ACE gene fragment. ACE activity increased by 2.5-fold in the ACE transfected ventricle as shown in the lower right panel of Color fig. 2.

Color fig. 3 shows the results of in situ TUNEL 3 weeks after ACE transfection. The left 2 panels show that there are TUNEL positive myocytes as indicated by arrows in the ACE transfected heart, but no positive myocytes in the LacZ introduced heart. The right panel shows the apoptosis related gene expression. Bax and bcl-2 remained unchanged, but mRNA levels of Fas/FasL, bcl-x L and caspase 1, 2 and 3 were enhanced in the ACE transfected heart shown in red compared with LacZ transfected heart. These findings suggest that cardiac ACE

could induce apoptosis independently of circulating neurohumoral factors and mechanical stress.

Inhibition of cardiac RAS can cause suppression of the remodeling process. We examined the effects of long-term treatment with enalapril and angiotensin receptor blockers ARB, TCV-116 on the cardiac remodeling process in BIO. The photomicrographs show 20-week-old BIO myocardia treated with a placebo, enalapril or TCV-116 for 15 weeks. Histological findings indicated that enalapril and TCV-116 reduced PAS-positive interstitial fibrosis. The myocytes are smaller and more densely located in the treatment group than in the placebo-treated group. Fibrous tissue volume was decreased in both treatment groups and much more decreased in the enalapril treated group. Numeric myocyte density was increased in both treatment groups and much more increased in the TCV treated group. ACE inhibitors potentiate bradykinin, prostaglandin and NO production besides inhibition of angiotensin II production. Because the LMMA treatment partially inhibited the improvement of fibrosis by enalapril, we consider that nitric oxide as

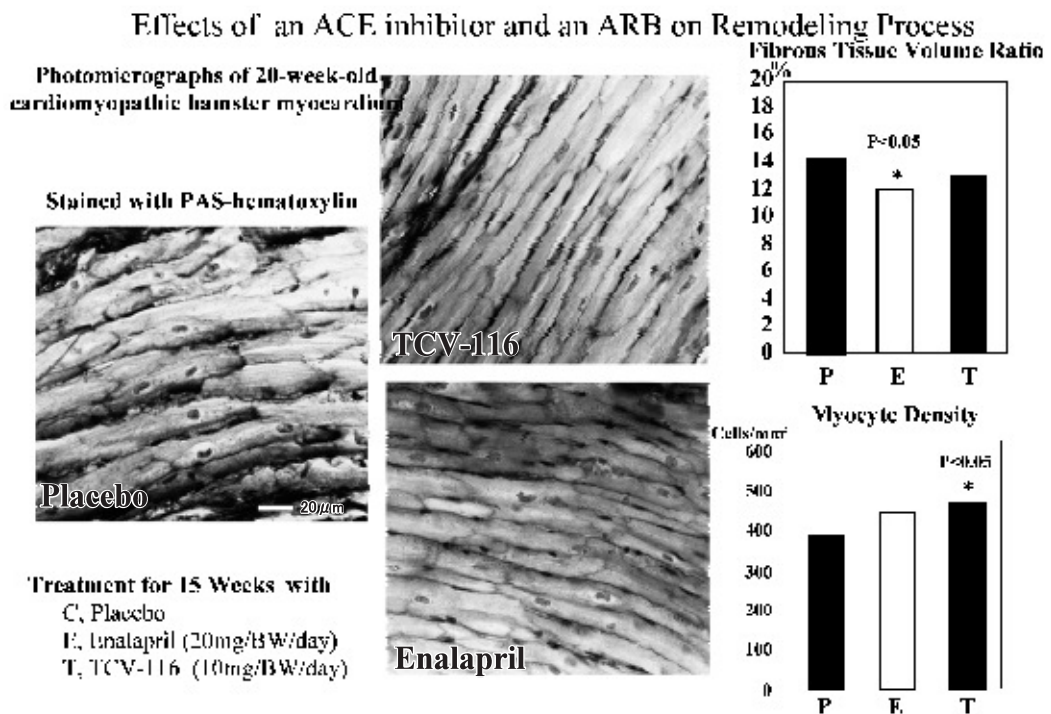


Figure 6 Left Panel: Photomicrographs of left ventricular sections in groups treated with TCV-116 (T) and enalapril (E) for 15 weeks were compared with that in untreated TO2 hamsters (P). Sections are stained by PAS-hematoxylin. Right Panel: Fibrous tissue volume ration and myocytes nuclear density in groups treated with TCV-116 (T) and enalapril (E) for 15 weeks were compared with that in untreated TO2 hamsters (P). Values are expressed as mean \pm SD. P: untreated TO2 hamster. T: TO2 hamster treated with TCV-116, E: enalapril. *p<0.05, compared with untreated TO2 hamsters.

well as angiotensin II are involved in the cardiac fibrosis (figure 6). These findings suggest that ACE inhibitors may exert different effects on cardiac remodeling from angiotensin receptor blockers.

We examined the synergistic effects of adding an ARB, valsartan to enalapril on survival in BIO. BIO treated with combination therapy had a significantly higher survival rate than those treated with a placebo or enalapril^{19) 22)}. The 500-days survival rates of hamsters treated with placebo, enalapril and the combination were 0%, 17% and 64%, respectively. These results showed that combination therapy with enalapril and valsartan had beneficial effects on prognosis. The synergistic effects of adding valsartan to enalapril on cardiac function and remodeling process. There was no difference in LVSP between the enalapril and the combination group. LV end-diastolic dimensions (LVDD) were lower in both treatment groups, and was much lower in the combination group. Myocyte density increased in the both treatment groups, and was more increased in the combination group. Myocyte density was corresponding to the percent fractional shortening. Doppler-echo cardiography revealed that E/A decreased in the both treatment groups, Corresponding to the %fibrosis.

In conclusion, our *in vivo* studies suggest that

- 1) cardiac RAS activation is involved in the remodeling process through myocyte cellular hypertrophy, an increase in fibrosis and myocyte apoptosis and that persistent activation of cardiac RAS might cause further progress in heart failure.
- 2) cardiac RAS inhibition exerts beneficial effects on the remodeling process leading to improvement of prognosis.

3. Cardiac Remodeling and Microvasculature

Introduction

The essential functions of the heart are performed at the level of the microvasculature, where oxygen, nutrients and hormones are delivered and catabolites are removed. Cardiac remodeling may result in abnormalities of the microvasculature and impaired angiogenesis after myocyte loss could participate in the process of cardiac remodeling. However, abnormalities in microvasculature and neovascular formation in the process of cardiac remodeling and the relationship between angiogenesis and cardiac remodeling have not been elucidated in DCM and heart failure. We hypothesized that alterations in microcirculation, especially in capillary microvasculature might be related to the progress of remodeling process. Accordingly, the goals of the present study were (1) to clarify the relationship between the progress in cardiac remodeling and alterations in capillary microvasculature leading to progressive deterioration in cardiac function and (2) to investigate the effect of pharmacological treatment on the capillary microvasculature and cardiac angiogenesis in dilated cardiomyopathy.

Materials and Methods

TO2 hamsters of three aged groups (5 weeks, 10-13 weeks, 20-23 weeks, n=10 respectively) were prepared for the experiments of capillary density, nuclear myocyte density and Northern blot analysis for procollagen type I and III, and transforming growth factor (TGF beta-1), compared with age-, sex-matched Flb hamsters (n=10, respectively). At the age of 5 weeks, 48 male TO2 hamsters were randomly assigned to receive either MCI-154 (5mg/kg/day, PO; n=12), or nifedipine (10mg/kg/day, PO; n=12), or amlodipine (10mg/kg/day, PO; n=12), or standard chow (control, n=12) for 15 weeks. MCI-154 was obtained from Mitsubishi pharmaceutical Co. (Tokyo, Japan) and amlodipine from Pfizer Co. (Tokyo, Japan).

Previous reports have shown that histochemical staining with the lectin Griffonia simplicifolia (GSA-B4) is a sensitive and reliable method to visible the entire capillary vasculature within the skeletal and cardiac muscle of hamster. Accordingly, LV sections from the present study were stained with GSA-B4 (Sigma Chemical Co., St. Louis, Mo, USA) in order to examine the morphology of the capillary bed. Hearts were removed and dipped into O. C. T compound (Tissue-Tek™, Sakura Finetechnical Co., Inc., Tokyo, Japan), and then frozen in liquid nitrogen and stored at -80C until use. Sections 8μm thick were obtained from cross-sections taken at the widest part of the left ventricle by means of cryostat. Sections were fixed with acetone for 10 min and air-dried and placed in phosphate-buffered saline (PBS) two times for 15 min. Then sections were treated with 3% hydrogen peroxide in methanol for 15 min to inhibit the activity of intrinsic peroxidase, and then washed two times for 5 min in PBS. GSA-B4 conjugated to biotin (0.2mg/ml, Sigma) was diluted 1: 100 in PBS and incubated on the tissue sections for overnight. The sections were then reacted with streptavidin conjugated to peroxidase (Nichirei, Co., Ltd., Tokyo Japan) for 5 min and thoroughly rinsed in PBS two times for 5min. Sites of bound lectin were visualized by incubation in a 3,3'-diaminobenzidine (DAB)-hydrogen peroxide substrate medium (Nichirei) for 5 min followed by two additional rinses. In order to enhance DAB reaction, the sections were rinsed with 0.05 M sodium bicarbonate (pH 9.6) for 10 min and then incubated in DAB Enhancing Solution (Vector Laboratories, Inc. Burlingame, USA) for 15 seconds. After counterstaining with hematoxylin, the tissue sections were dehydrated through a graded series of ethanols and xylenes and coverslipped. Using with light microscopy (PM-10AK, Olympus Co., Ltd., Japan) and camera (C-35AD, Olympus). Numbers of coronary capillaries and the nuclei of cardiomyocyte were counted in 11.25 mm² area per a section. Sections 16μm thick were obtained from cross-sections taken at the widest part of the left ventricle. Double staining of sections for discriminating arteriolar and venular capillaries was performed. Arteriolar capillaries were stained blue, because they contained alkaline phosphatase and venular capillaries were stained red because they contained dipeptidylpeptidase IV, and intermediate capillaries were stained violet because they contained both enzymes. Capillaries and myocytes were drawing tube

attached the microscope. The ratio of venular capillaries to total capillaries and proportion of venular capillaries were calculated.

Northern blot analysis

The cDNA probes used in the present study were cDNA for human procollagen type I (Hf 677), type III (Hf 934), rat TGF-beta1 (ATCC, RI 95-03, 63197), and glyceraldehyde-3-phosphate dehydrogenase (GAPDH) (#57091, American Type Culture Collection Rockville, Md) as an internal control. All cDNA probes were uniformly labeled with random primers using Klenow enzyme (Boehringer Mannheim) and α -³²P-dCTP (Life Science Products). Each preparation of total RNA was isolated from a left ventricular tissue sample using TRIzol™ reagent (GIBCO BRL). Twenty micrograms of denatured RNA was size-fractionated on 2% formaldehyde-1.2~1.5% agarose gels and then transferred onto a nylon membrane (Hybond-N+™, Amersham Life Science) overnight using saline sodium citrate transfer buffer. Northern blot analysis was carried out according to the established method. Each membrane was exposed at -80°C on X-ray films (X-OMAT, Eastman Kodak) with a single intensifying screen for increasing exposure times to obtain signals in the linear range for densitometric analysis of each mRNA species. The GAPDH mRNA diffuse density score used as an internal control has been shown to be unchanged in the different ages of DCM hamster heart. To evaluate mRNA levels, an optical scanner (GT-9500, Seiko, Tokyo, Japan) was utilized to digitize autoradiograms. The density of autoradiogram bands in the digitized image was measured with the use of the public domain NIH Image program and a computer (Macintosh Performa 6310, Apple Computer, USA).

Morphometric analysis and immunohistochemical staining

Basic FGF and VEGF were immunohistochemically stained using an anti-bovine bFGF antibody (Upstate Biotechnology Inc., USA) and an anti-human VEGF antibody (Santa Cruz Inc., USA), visualized with biotinized anti mouse IgG and aminoethylcarbazole (ACE substrate kit, NItirei, Tokyo).

Results

Capillary

The total capillary density was counted by biotin-labeled lectin method. The total capillary density in TO2 hamster was not different from that in F1b at the age of 5 weeks ($3019 \pm 171/\text{mm}^2$ vs $2977 \pm 219/\text{mm}^2$, NS), but decreased significantly at the ages of 13 and 20 weeks compared with the F1b (13weeks; $1879 \pm 312/\text{mm}^2$ vs $2243 \pm 177/\text{mm}^2$, $p < 0.01$, 20 weeks; $1268 \pm 183/\text{mm}^2$ vs $1963 \pm 259/\text{mm}^2$, $p < 0.01$). Double staining of sections for discriminating arteriolar and venular capillaries showed a decrease in proportion of venular capillary at the age of 20 weeks in TO2.

Effects of Treatments with nifedipine, amlodipine and MCI-154

Micrographs of cardiac cross-sections of TO2 treated with and nifedipine (N),

amlodipine (A) and MCI-154 (M) were compared with untreated. Treatment with (A) and (M) revealed that myocyte hypertrophy, myocytolysis and increase in interstitial space were attenuated. In groups treated with (A) and (M), LVDD was decreased ($p < 0.01$) and %FS was increased ($p < 0.001$) at the age of 20 weeks compared with untreated TO2, whereas nifedipine had no effect on echocardiographic parameters. Treatment with (A) decreased tau significantly. In groups treated with (A) and (M), IRT and DT significantly reduced to the level of F1b hamsters. Total capillary density was significantly increased both in (A) and (M). Proportion of venular capillary and VEGF mRNA expression levels increased both in (A) and (M). The relative ratio of mRNA expression of VEGF to GAPDH obtained from densitometric scanning among three groups. Immunohistochemical staining for bFGF revealed that brownish-red staining represents extracellular bFGF visualized with anti-mouse IgG and aminoethylcarbazole. The manifestation of bFGF and VEGF were stronger in TO2 treated with both in (A) and (M). Brownish-red staining represents VEGF in cardiac myocytes. Basic FGF and VEGF was not manifested in untreated TO2 and F1b. In a nifedipine-treated group, there were no significant alterations in all the above parameters including micrographic changes.

Discussion

We used TO2 strain as the model of DCM. It is well established that the disease process affects myocardial tissue in greatly inhomogeneous ways as evidenced by focal cell loss, microvascular spasms, inhomogeneous capillary flow and resultant focal ischemic areas, marked heterogeneity in cellular calcium content⁸ due to enhanced phospholipid metabolism and abnormality in sarcoplasmic membrane permeability²³. Recently a defect in the genes for δ -sarcoglycan, dystrophin-associated glycoprotein, was reported in cardiomyopathic hamster²⁴. Beginning at approximately 30 days of age, the hamsters develop progressive myocytolytic necrosis in heart and skeletal muscle, and myocyte integrity is lost through slow loss of myofibrils and is replaced by amorphous material. Increases in the expressions of mRNA for collagen type I, type III and TGF- β 1, and decrease in the number of cardiomyocytes, were apparent at 13 weeks old, and then these cardiac remodeling progressed with age¹². The TO2 strain of cardiomyopathic hamsters was derived from Bio animals and shows severe fibrosis and dilatation of the left ventricle due to extensive focal myocytolytic necrosis, thus provide a uniform pathogenesis of DCM and a useful model for heart failure.

We hypothesized that inappropriate neovascularization could not supply enough blood to fit the demand for the remodeled myocardium in DCM and heart failure. Thus, the goals of the present study were to investigate whether angiogenesis is related to cardiac remodeling leading to progressive deterioration in cardiac function and to ascertain whether changes in microvasculature could be attenuated by the pharmacological treatment. The results are summarized as

follows. 1) Cardiomyopathic hamsters showed decreases in capillary density and proportion of venular capillaries concomitantly with a decrease in numerical myocyte density and enhanced gene expressions for collagen I, III and TGF- β 1 leading to cardiac fibrosis. 2) Long-term treatment with amlodipine and MCI-154 could suppress decreases in capillary density and proportion of venular capillaries concomitantly with induction of VEGF and bFGF.

In the present study, changes in myocyte density and collagen deposition were parallel to alteration in the total capillary density. Thus, alterations in cardiac microvasculature may concern with remodeling process. Various alteration in the structure and function of the microvasculature occur in most forms of heart disease. Tanganelli has demonstrated that thickening of the walls of pre-capillary arterioles and capillaries occurs due to increased deposition of endothelial and pericyte basement membranes in patients with DCM. Decreases in arteriolar density and coronary reserve have been reported in patients with HCM. Angiogenesis, the growth of new vessels, is a complex process involving both the proliferation and migration of endothelial cells. Myocardial ischemia may be a potent inducer of angiogenesis. However, there is insufficient evidence to establish a causal link with myocyte loss and neovascularization in DCM and heart failure. Coronary neovascularization might be strongly involved in cardiac remodeling. The extracellular matrix, its fibrillar collagen and myocyte hypertrophy could participate in cardiac remodeling. Diffusion distances from capillaries to myocytes increase due to fibrosis and coronary reserve is diminished, which may lead to deterioration in capacity to produce angiogenic cytokines such as VEGF in hypertrophied myocytes. Morphometric studies of human hearts indicate that in infancy myocardial capillary density is higher (3315/mm²) than in adults (2388/mm²) and that, in the young, there is a capacity for capillary angiogenesis in response to pressure overload hypertrophy, but this is lost or substantially diminished in the adult. In our data, the proportion of venular capillaries and ratio of venular capillaries to total capillaries were significantly lower than those in F1b hamsters. Both amlodipine and MCI-154 could suppress decreases in capillary density and proportion of venular capillaries concomitantly with induction of VEGF and bFGF. It has been demonstrated from the studies of metastatic carcinoma that capillary angiogenesis usually initiates from the venular site and an increase in the proportion of venular capillaries indicates the much more promotion of neovascularization. It is reported that cytokines inducible angiogenesis, such as bFGF and VEGF, are mainly produced from the ischemic or stretched myocytes¹⁵⁻¹⁶. Increased induction of bFGF and VEGF might show that myocyte preservation caused to recover the capacity to produce angiogenic cytokines and to improve cardiac performance by the treatment. The present study addressed potential unique effects of a newly developed Ca²⁺sensitizer, MCI-154 and a Ca²⁺antagonist, amlodipine. It is known that long-term treatments with MCI-154 and amlodipine might preserve cardiac performance by inhibition of Ca²⁺overload. Calcium

sensitization increases myocardial contractility by improving energy utilization of the myocardium, without an increase in intracellular concentrations of cyclic adenosine monophosphatase. Dehydropyridine derived Ca^{2+} antagonists prevent Ca^{2+} influx from Ca^{2+} -induced Ca^{2+} release, which is activated in the failing and remodeled myocardium. In contrast to amlodipine, nifedipine had neither effects on cardiac performance or remodeling. Regarding the difference between amlodipine and nifedipine, it is known that amlodipine has a kind of anti-oxidant action and exerts inhibitory effects on cytokine induction. Amlodipine and MCI-154 have been shown to exert beneficial on cardiac performance in acute and chronic cardiac dysfunction. However, this is the first report that long-term treatment of MCI-154 might exert beneficial effects on cardiac performance and remodeling process in DCM. Yet, exact mechanism responsible for angiogenetic action has not been elucidated in this experiment. It is not known which precede to improve the cardiac function, neovascularization or myocyte preservation. Because MCI-154 exerts a positive inotropic action without increasing myocardial oxygen and energy consumption, it might have a beneficial effect on cardiac remodeling, especially microvasculature and myocyte preservation. There is no evidence that both amlodipine and MCI-154 can directly affect the neovascularization.

As it has been suggested that changes in the vessel wall geometry and consequently wall tension induce growth of new vessel, it is possible that higher wall stress, concomitantly with increased blood flow induced by the amelioration of the diastolic function of LV, might produce slight damage to the capillary endothelium, which would lead to the release of protease, degradation of the basement membrane and subsequent endothelial migration and mitosis. There is a close correlation between left ventricular end diastolic pressure and capillary density in the cardiac tissue. Accordingly the improvement of cardiac performance evoked with MCI-154 may induce angiogenesis in LV of TO2.

In conclusion, 1) Alterations in capillary microvasculature might be involved in the process of cardiac remodeling of dilated cardiomyopathy. 2) Suppression of angiogenesis might be related to alterations in capillary microvasculature. Induction of cardiac angiogenesis might be a new strategy for the treatment of remodeling process in dilated cardiomyopathy.

4. Immunological Activation and Intervention in the Failing Myocardium

4-1. Blockade of CTLA4Ig and Heart Failure

Introduction

A number of pro-inflammatory cytokines as well as neurohumoral factors are activated in heart failure. Various stimuli, including autoimmunity, chronic infections, mechanical overload, and ischemia, induce production of inflammatory cytokines as shown in figure 7. These cytokines further negatively influence contractility and contribute to the remodeling process in the failing myocardium

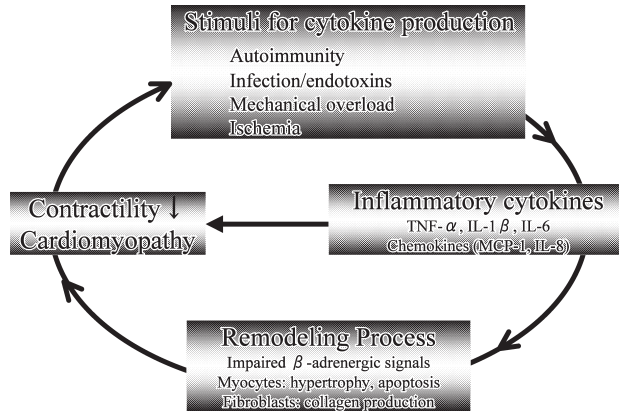


Figure 7 Schematic View modified Damas JK. et al. (Curr Control Trials Cardiovasc Med 2001; 2: 271)

resulting in heart failure. Recently, it has been reported by Douglas Mann and his colleagues that TNF- α inhibition with a recombinant chimeric soluble TNF- α receptor, etanercept, causes a significant dose-dependent improvement in the ejection fraction as shown in panel A, as well as improvements in left ventricular end-diastolic volume, end-systolic volume, and left ventricular volume, respectively. Etanercept also improves functional status. Using etanercept, RENAISSANCE and RECOVER randomized over 1500 patients. However, the RENEWAL study, of which RENAISSANCE and RECOVER were the constituent parts, was stopped because of the lack of evidence of beneficial effects. Clinically tried treatment regimens of immuno-modulation are summarized. Anti-cytokine treatments might only be relevant to targeting cytokines during the time of inflammation. Immunosuppressive drugs cause side effects, increase the risk of infection, and are associated with neoplasms along with the benefits. Immunoabsorption has been found to improve functional capacity in DCM patients. There are pros and cons about the effects of immunoglobulin on cardiac function. However, the results of these small studies have to be confirmed in larger, placebo-controlled mortality and morbidity studies. Thus, even now, immuno-modulation therapy remains controversial in heart failure. Seko reported that antigen-specific T cells, perforin-expressing cytotoxic lymphocytes and natural killer cells infiltrated the heart concomitantly with expression of B7-1, B7-2, and CD40 in the cardiac myocytes of patients with acute myocarditis and DCM. This raises the possibility of immunotherapy to prevent T-cell-mediated as well as NK cell-mediated myocardial damage in myocarditis and DCM. On the other hand, it has been demonstrated that T cell-mediated autoimmunity may cause DCM. PD-1, which is one of the costimulatory molecules leading to the negative regulation of the T cell response, and its deficiency in BALB/c mice caused DCM. In PD-1 KO mice, the heart was enlarged and the wall motion was diffusely reduced. Affected hearts showed

diffuse deposition of IgG on cardiomyocytes. All of the PD-1 knock-out mice exhibited high-titers of circulating IgG autoantibodies. These results indicate that blockade of costimulatory molecules is a potent strategy contributing to the prevention of autoimmune heart diseases. T cells require two distinct signals for their full activation. The first signal is provided by the engagement of the T cell receptor (TCR) with MHC on antigen-presenting cells (APCs), and the second costimulatory signals are provided by engagement of one or more T-cell surface receptors with their ligands on APCs. Among the costimulatory signals, CD28/CTLA4 and B7 have major roles in the T cell activation. CTLA4IgG effectively inhibits this ligation as an immunoadhesin and induces antigen-specific T cell unresponsiveness. However, CTLA4IgG has a too-short half-life and needs repetitive administration (figure 8). It is hard to maintain efficient serum concentration.

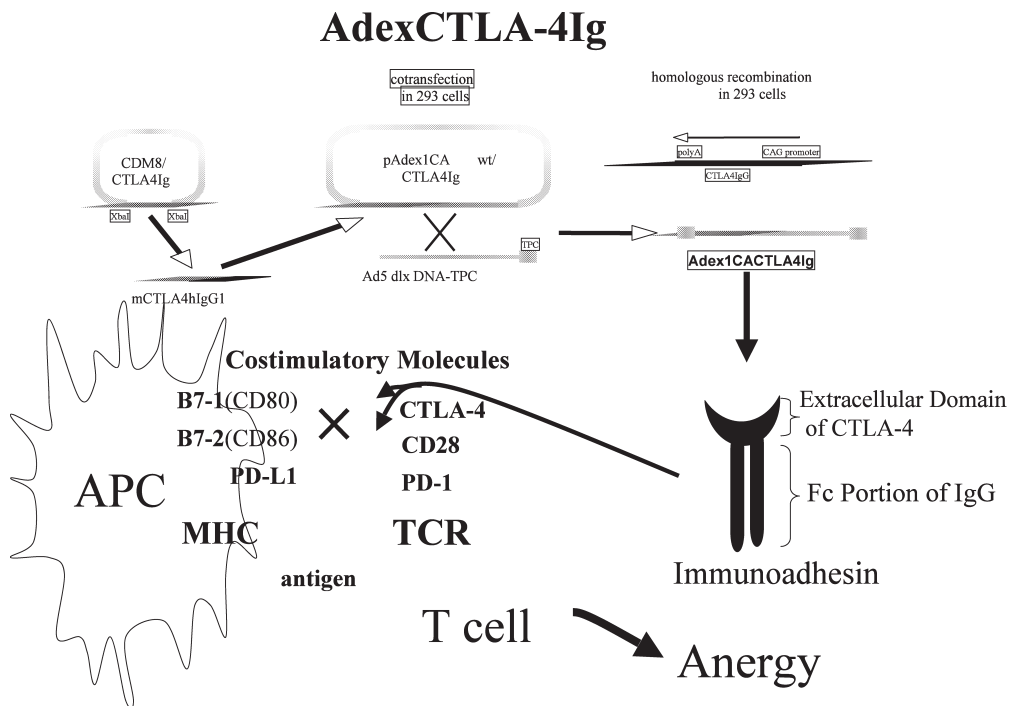


Figure 8 AdexCTLA4Ig was prepared by the method previously described for the construction of Adex1CACTLA4Ig (Nakagawa et al., 1998). Briefly, recombinant adenoviruses were constructed by in vitro homologous recombination in 293 cells by using pAdex1CAICOSIg and the adenovirus DNA terminal protein complex. The desired recombinant adenovirus, called Adex1CACTLA4Ig, was propagated in 293 cells and purified by two rounds of cesium chloride density centrifugation. The concentrated virus was dialyzed against phosphate-buffered saline (PBS)-10% glycerol. The titer of the virus stock was assessed by a plaque formation assay that used 293 cells. CTLA4IgG effectively inhibits this ligation as an immunoadhesin and induces antigen-specific T cell unresponsiveness.

Thus, we have constructed recombinant adenovirus AdexCTLA4Ig as shown in the upper panel. As shown in the left panel of Color fig. 4, the serum concentration of CTLA4Ig was dose-dependent and decreased gradually, but was still maintained at an efficient dose even 180 days after only one iv administration of AdexCTLA4Ig. Adex-mediated gene expression occurs mainly in liver cells. The right panel on days 14 and 42 after treatment with AdexCTLA4Ig shows that sinusoidal cells and hepatocytes were stained with antibody against the Fc portion of human IgG. Thus, it was demonstrated that the hepatic expression of AdexCTLA4Ig was persistent and efficient *in vivo* to maintain the serum concentration. The use of recombinant adenoviruses for gene therapy has been limited by host immune responses in part due to cytotoxic lymphocyte activation. In fact, as shown in panel A of figure 9, many inflammatory cells and apoptotic hepatocytes, shown by white arrowheads, were detected in the liver inoculated with AdexACE or Adex-LacZ. In contrast, there is little if any inflammatory response in the liver after AdexCTLA4Ig administration, as shown in panel B. In general, these host immune

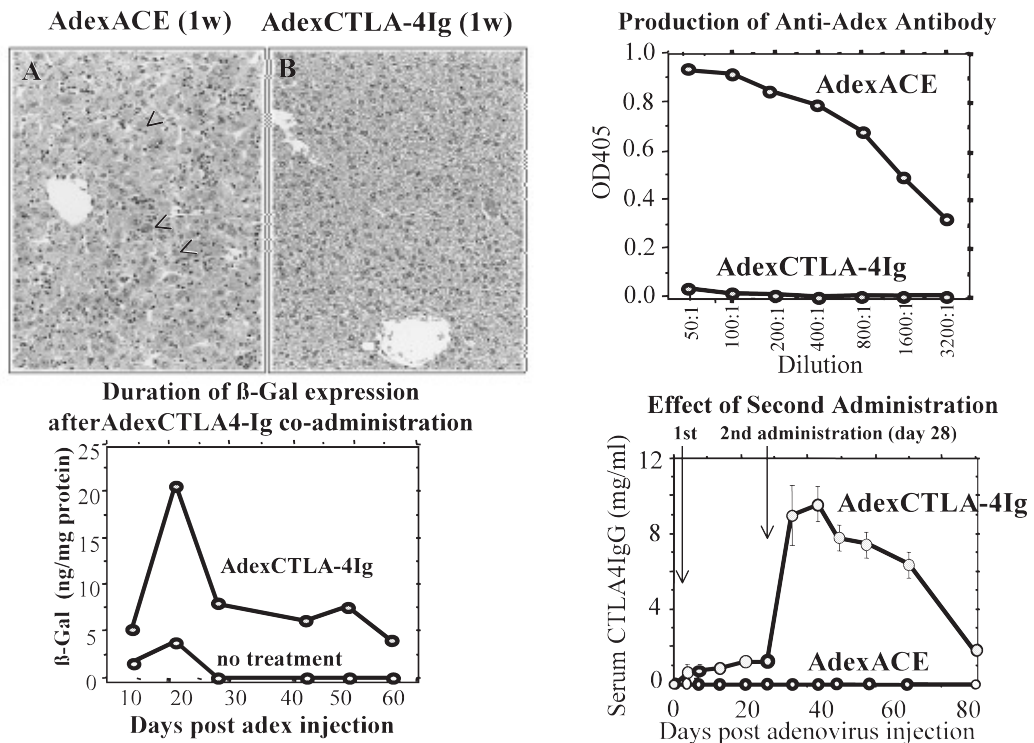
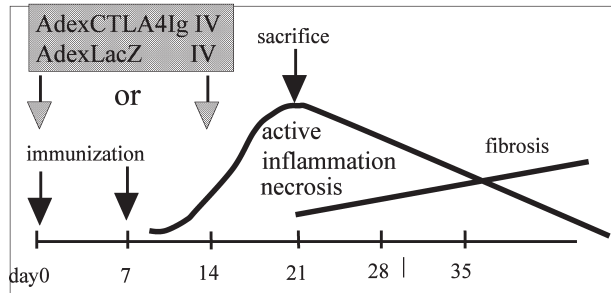


Figure 9 In mice pre-inoculated with AdexACE showed an increase in anti-adenovirus antibody production. AdexCTLA4Ig completely blocked the production of anti-adenovirus antibody. In addition, as shown in the right lower panel, the serum concentration of CTLA4Ig was significantly elevated after the second administration in mice pretreated with AdexCTLA4Ig. On the other hand, serum CTLA4Ig could not be detected in mice pretreated with AdexACE because of antibody production.

responses are partly because of anti-adenoviral antibody production. In mice pre-inoculated with AdexACE showed an increase in anti-adenovirus antibody production. However, AdexCTLA4Ig completely blocked the production of anti-adenovirus antibody (figure 9). In addition, as shown in the right lower panel of figure 13, the serum concentration of CTLA4Ig was significantly elevated after the second administration in mice pretreated with AdexCTLA4Ig. On the other hand, serum CTLA4Ig could not be detected in mice pretreated with AdexACE because of antibody production. Thus, AdexCTLA4Ig alone can completely prevent anti-adenovirus antibody production *in vivo* leading to a persistent and efficient serum concentration of CTLA4Ig. Next, we examined whether co-administration with AdexCTLA4Ig induced persistent gene expression by another adenovirus. Administration of AdexCTLA4Ig prolonged AdexLacZ-mediated gene expression in the liver for over 70 days as shown in the left lower panel of figure 9. This co-administration will be useful in human gene therapy using various types of virus vectors that subsequently elicit antiviral immune responses. Next, as to the applications of this AdxCTLA4Ig in the experimental model. First, we examined the effect of AdexCTLA4Ig before and after the onset of experimental autoimmune myocarditis (EAM). EAM is transferable into syngeneic rats not by antibodies but by activated T cells. However, the effect of T cell activation blockade on the prevention of EAM was unknown. The clinical course of EAM and experimental protocols are schematically shown in figure 10. Male Lewis rats were immunized subcutaneously twice with porcine cardiac myosin on days 0 and 7. A focal inflammation, mainly of macrophages, was detected in the myocardium and this initial inflammatory phase lasted up to day 14. Thus, AdexCTLA4Ig or AdexLacZ as a control was injected intravenously on days 0 and 14. Twenty-five percent of EAM rats treated with AdexLacZ died, whereas no rats died in the AdexCTLA4Ig-treated groups. All dead rats showed macroscopic evidence of severe myocarditis and heart failure. RT-PCR revealed that costimulatory molecule mRNA expression of B7-1, B7-2, CD28, CD40, and CD40L was enhanced in the AdexLacZ-treated EAM rats. Moreover, enhanced expression of B7-1, B7-2, and CD40 were observed on cardiac myocytes. Thus, myocytes as APCs may play a critical role in the engagement with the T cells. Representative views of macroscopic and microscopic findings of cardiac tissues after treatment on days 0 and 14 are shown in Color fig. 5. All rats treated with AdexLacZ showed discoloration of the surface and cardiac enlargement, and developed typical severe autoimmune lesions composed of inflammatory cells including giant cells, macrophages, lymphocytes, and degenerated myocardial tissue. On the other hand, no rats in the AdexCTLA4Ig-treated groups on day 0 showed abnormalities macroscopically and there was very little infiltration of inflammatory cells, if any, in the myocardium. In a group treated with on day 14, minimal myocarditis was observed 7 days after treatment. As shown in the upper panel of figure 11, the heart weight to body weight ratios in groups treated with AdexCTLA4Ig on days 0 and 14 were significantly lower than

Experimental Autoimmune Myocarditis (EAM)



(Okura Y, et al. J. Mol. Cell. Cardiol. 1997; 29: 491-502)

Figure 10 Experimental autoimmune myocarditis (EAM) is transferable into syngeneic rats not by antibodies but by activated T cells. The clinical course of EAM and experimental protocols are schematically shown. Male Lewis rats were immunized subcutaneously twice with porcine cardiac myosin on days 0 and 7. A focal inflammation, mainly of macrophages, was detected in the myocardium and this initial inflammatory phase lasted up to day 14.

HW/BW and Affected Area Ratio

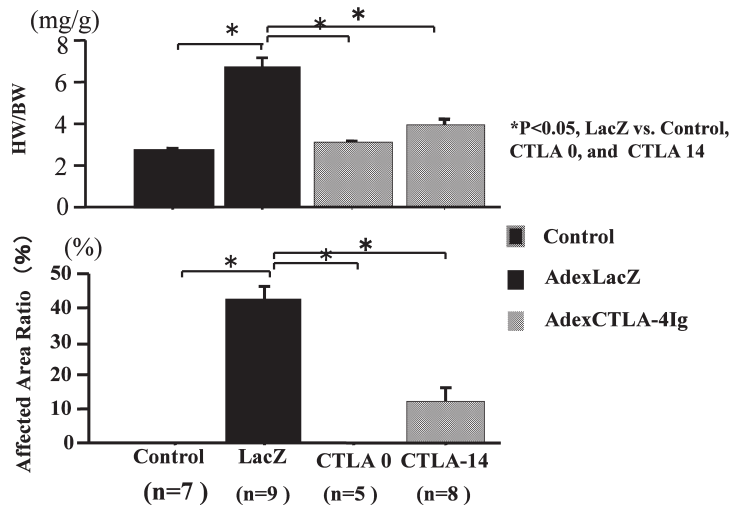


Figure 11 HW/BW and Affected Area Ratio in groups control, LacZ, CTLA4Ig on day 0 and 14.

those of AdexLacZ-treated EAM rats and almost equivalent to those of normal rats. The affected area ratio of AdexCTLA4Ig-treated group on day 0 was almost completely inhibited and in treated groups on day 14, the affected area was significantly reduced. These findings indicate the clinical benefits of adenovirus-mediated costimulatory signal blockade after the onset of myocarditis. Figure 12 shows the mRNA expression of several cytokines. Moderate to strong expression of Th1-type cytokines such as IL-2 and IFN- γ , proinflammatory cytokines such as IL-1 β , TNF- α and IL-6, and Th2-type cytokines such as IL-4 and IL-10, was detected within the hearts on day 21 in the myocardium after injection of AdexLacZ as shown by the black bars, whereas the expression of these cytokines was almost completely inhibited on day 21 after injection of AdexCTLA4Ig as shown by the red bars. This study demonstrates that blockade of T-cell costimulatory signals using adenovirus vectors containing CTLA4Ig could prevent both the onset and the progression of EAM. Next, we tested the effect of AdexCTLA4Ig on cardiac graft survival. Fetal Donor hearts of B6 mice were implanted into the recipient auricular of CBA/J mice, to which AdexCTLA4Ig or

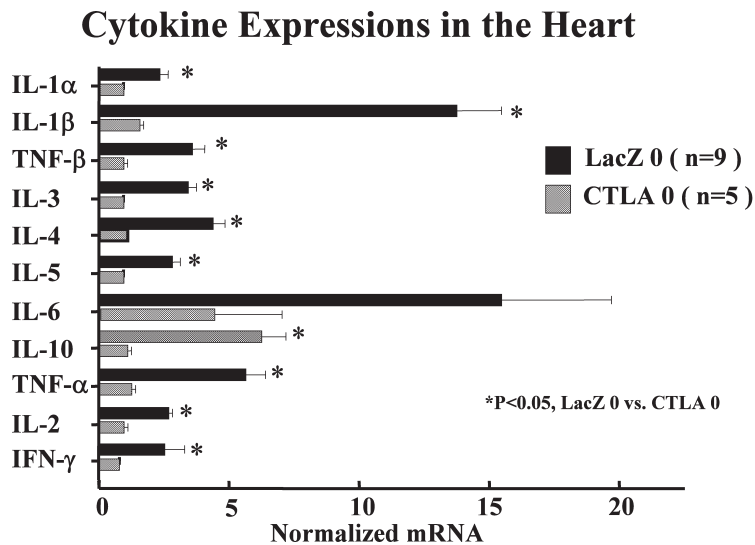


Figure 12 Effects of AdexCTLA4Ig treatment on antigen-specific cytokine production. Lymph node cells were obtained on day 21 after immunization from normal rats (n=6) or EAM rats treated with Adex-LacZ day 0 (n=7), AdexCTLA4Ig day 0 (n=5). The cells were cultured with or without 100 pmol/ml of porcine cardiac myosin. Supernatants were collected and IFN- γ (A), TNF- α (B), IL-1 β (C), and IL-4 (D) levels in the supernatants were determined by means of ELISA. Values represent mean \pm SE. * P<0.05 vs. AdexLacZ day 0.

AdexLacZ was administered one week before implantation. Graft survival was determined by ECG monitoring. As shown in figure 13, all the grafted hearts were rejected within 14 days in the group without AdexCTLA4Ig treatment, but cardiac allograft survival was prolonged in the group treated with AdexCTLA4Ig. It is suggested that inflammatory mediators released due to ischemia-reperfusion injury lead to the immune response by upregulating MHC class II in the peripheral T lymphocytes. We developed an in-vivo system, in which AdexCTLA4Ig or AdexLacZ was injected via a recipient vein 5 days before transplantation. In human heart transplantation, average ischemic times are between 3 and 4 hours. Thus, we set the ischemic time at 4 hours adding to the procedure and investigated the protective effect of CTLA4Ig against the immune response caused by reperfusion after transplantation. Hearts were transplanted into a heteropoeitic location in recipients after ischemia in St. Thomas solution for 4 hours. As shown in Color fig. 6, 4 hours of ischemia after pretreatment with AdexLacZ resulted in over 40% infarcted area as determined by triphenyl tetrazolium chloride (TTC) staining and over 30% affected area, evaluated on the basis of the extent of inflammatory cell infiltration. Pretreatment with AdexCTLA4Ig reduced the size of the infarcted

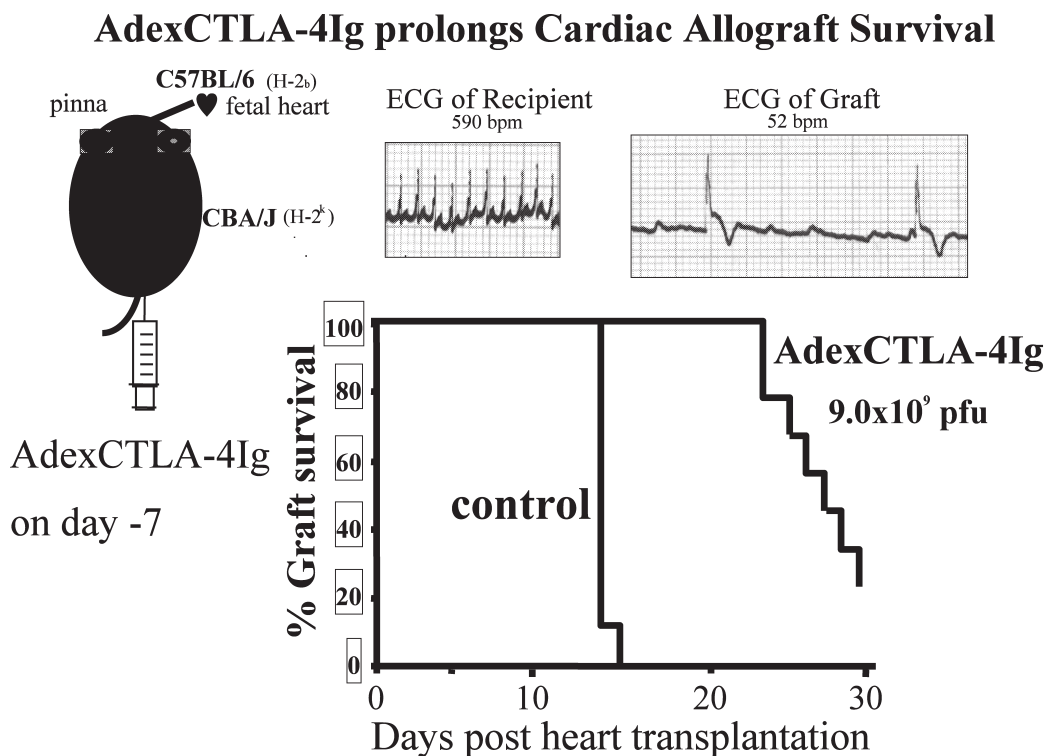


Figure 13 The effect of AdexCTLA4Ig on cardiac graft survival. Fetal Donor hearts of B6 mice were implanted into the recipient auricular of CBA/J mice, to which AdexCTLA4Ig or AdexLacZ was administered one week before implantation. Graft survival was determined by ECG monitoring.

area and affected area. Thus, the adenovirally mediated gene transfer of CTLA4Ig attenuated the reperfusion injury in a rat syngenic cardiac transplantation model. The left 2 panels of Color fig. 7 show representative in situ TUNEL findings with AdexCTLA4Ig or AdexLacZ pre-treatment.

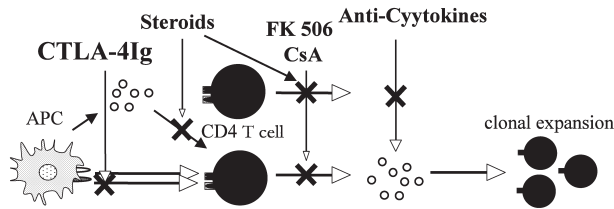
Without treatment of AdexCTLA4Ig, severe inflammatory cell infiltration and few but significant myocytes apoptosis were caused, whereas, pre-treatment with AdexCTLA4Ig suppressed inflammation and diminished Tunel-positive cells. The right panel shows the apoptosis-related gene expression by multi-probe RPA. Messenger RNA levels of Fas/FasL, bcl-x L and caspase 1, 2 and 3 were enhanced in hearts with AdexLacZ pre-treatment shown by red bars compared with AdexCTLA4Ig pre-treatment as shown by white bars. The mechanism whereby CTLA4Ig afforded protection from IRI could involve not only inhibition of the immune response, but also increased resistance of cardiomyocytes to apoptosis. In the clinical application, the long lasting CTLA4Ig expression may cause a problem in humans, who may not be able to mount immune responses against various bacterial and viral insults after AdexCTLA4Ig administration. To overcome this problem, we constructed a new adenovirus vector that contained the Cre-loxP system. Using this system, AdexCTLA4Ig expression was terminated as shown in panel B, serum concentration of CTLA4Ig could not be detected, and production of CTLA4Ig in liver was stopped as shown in panels D and E of Color fig. 8. This new type of vector enabled us to terminate the in vivo gene expression at the desired time. Steroids, cyclosporine A and FK506 act by impairing T cell receptor signal transduction, which lead to pan-T cell suppression including antigen-specific T cells. On the contrary, CTLA4Ig block specifically the costimulatory signal when antigen was presented. Potential treatment modalities of AdexCTLA4Ig are summarized in figure 14. Our study indicates the therapeutic potential of the gene-transfer method in myocarditis, cardiac transplantation and ischemia-reperfusion injury after cardiac transplantation.

DCM in relation to autoimmune mechanisms, and in other T-cell-mediated autoimmune heart diseases may be on the same line. In addition, blockade of T cell costimulatory signals might be an efficient and helpful tool when heart and bone marrow derived stem cell are transplanted, in which autoimmunity could be induced. However, therapeutic strategies might be influenced by the underlying disease, etiology, stage and extent of its attribution as shown by the former studies. Prolongation of other gene expressions using various types of virus vectors may be relevant in human gene therapy.

4-2. ICOSIgG and EAM

To achieve effective inhibition of the costimulatory pathway, we have constructed recombinant adenovirus AdexICOSIg containing the extracellular domain of human ICOS and the Fc portion of human immunoglobulin G1. We examined the effects of these adenovirally delivered fusion proteins on the prevention of EAM

Potential Treatment Modalities in Heart Failure



Anti-cytokine-sTNFR, IL-1R antagonist, IL-10, Pentoxifylline
 Chemokine modulators
 Intravenous Immunoglobulin
 Immunosuppressive Therapy - Steroids, CsA, FK506
 Plasmapheresis-Immune complex, autoantibody
 Immunoadhesin -Etanercept, CTLA4Ig, AdexCTLA4Ig

Figure 14 Schematic view of potential treatment modalities in heart failure

in the T cell activation phase and the initial inflammatory phase.

In this study, we demonstrated that (1) the expression of ICOS/ICOSL molecules was enhanced in the lymph nodes, spleen, and heart of the EAM rat compared with normal rats. (2) AdexICOSIg treatment on day 0 did not significantly inhibit the onset of EAM. (3) On the other hand, delayed treatment with AdexICOSIg strikingly inhibited the ongoing EAM. (4) Blockade of the ICOS/ICOSL pathway significantly inhibited antigen-specific lymph node cell proliferation by impairment of interaction between antigen-presenting-cells and memory/effector T cells. This study indicates that ICOS/ICOSL costimulation makes an important contribution to the progression of EAM and that blockade of this pathway by gene transfer has therapeutic potential for ongoing human myocarditis. Male Lewis rats, 6-8 weeks of age, were purchased from Japan Charles River (Yokohama, Japan) and maintained in our animal facilities. Cardiac myosin was prepared from the ventricular muscle of the porcine heart according to the methods previously described²⁵⁾ and used as an antigen.

In experiment 1, male Lewis rats were immunized subcutaneously twice with 2 mg of cardiac myosin in an equal volume of complete Freund's adjuvant (CFA; Difco Laboratories, Detroit, MI, USA) supplemented with mycobacterium tuberculosis R37a (Difco Laboratories, Detroit, MI, USA) at a concentration of 11mg/ml on days 0 and 7.

In experiment 2, to study the effects of AdexICOSIg on the severe form of EAM, male Lewis rats were immunized subcutaneously twice with 4 mg of cardiac myosin in an equal volume of CFA supplemented with mycobacterium tuberculosis R37a at a concentration of 11mg/ml on days 0 and 3. A murine anti-rat ICOS monoclonal antibody (MAb) was obtained from JT Inc., Yokohama, Japan²⁶⁾. A goat anti-rat

GL50 polyclonal antibody (PAb) specifically recognizing rat ICOSL was purchased from Santa Cruz Biotechnology (Santa Cruz, CA, U. S. A). In this study, to amplify the specific signals of the antigen-antibody reaction, we applied a two-step immunohistochemistry procedure with high sensitivity based on labeled polymers. The heart samples from normal rats and EAM rats, which were immunized according to the protocol described in experiment 1 and sacrificed on day 21 after immunization, were snap frozen in OCT compound and used for cryosections. Six-micrometer-thick cryosections were picked up on slides and air dried. Sections were fixed in acetone for 10 min and air dried for at least 10 min. Sections were then incubated for 60 min at 20°C with the anti-rat ICOS MAb or anti-rat ICOSL PAb. After washing in PBS, slides were covered with DAKO En Vision+ goat anti-mouse Ig peroxidase (Dakopatts, Copenhagen, Denmark) supplemented with 3% normal rat serum for 30 min at 20°C, or with DAKO LSAB+biotinylated porcine anti-goat Ig (Dakopatts, Copenhagen, Denmark) for 10 min at 20°C followed by peroxidase-conjugated streptavidin for 10 min at 20°C. After washing with PBS, the slides were stained for peroxidase activity with 3,3'-diaminobenzidine tetrahydrochloride. Sections were counterstained with Mayer's hematoxylin. The inguinal and popliteal lymph nodes and spleen were aseptically removed from normal rats and EAM rats, which were immunized according to the protocol described in experiment 1 without administration of the adenovirus and sacrificed on day 21 after immunization. Lymph node cell suspensions were prepared by passage through a 200-gauge stainless steel mesh. Then cells were washed twice in RPMI 1640 medium with 10% fetal bovine serum. They were incubated with a mixture of phycoerythrin-labeled W3/25 (CD4, PharMingen, San Diego, CA, USA), OX-8 (CD8, PharMingen), CD25 (PharMingen), CD45RA (a B cell marker; PharMingen), or a macrophage subset (PharMingen), and FITC-labeled ICOS (JT-Inc.) or ICOSIg followed by FITC-labeled anti-human IgG1 (Zymed). A total of 20000 cells were analyzed by FACScan flow cytometry (Becton Dickinson). Dead cells were excluded by propidium iodide gating. AdexICOSIg was prepared by the method previously described for the construction of Adex1CACTLA4Ig⁸⁾ except that the CTLA4Ig fragment was replaced with cDNA of human ICOSIg. Briefly, recombinant adenoviruses were constructed by in vitro homologous recombination in 293 cells by using pAdex1CAICOSIg and the adenovirus DNA terminal protein complex. The desired recombinant adenovirus, called Adex1CAICOSIg, was propagated in 293 cells and purified by two rounds of cesium chloride density centrifugation. The concentrated virus was dialyzed against phosphate-buffered saline (PBS)-10% glycerol. The titer of the virus stock was assessed by a plaque formation assay that used 293 cells. Serum concentrations of ICOSIg were assayed by competitive-enzyme-linked immunosorbent assay (ELISA) as previously described⁸⁾. Briefly, sample sera were collected periodically from the retro-orbital plexus of rats. Purified ICOSIg was coated onto 96-well plates. A diluted serum sample or standard ICOSIg with rabbit anti-ICOSIg antiserum was added to the BSA-blocked

wells. After washing, a peroxidase-labeled goat anti-rabbit antibody (Jackson Immunoresearch Lab, Bar Harbor, ME, USA) was added. Finally, the substrate o-phenylenediamine-H₂O₂ was added and absorbance at 490 nm was measured. Each sample was analyzed in duplicate. In experiment 1, 5.0×10^9 plaque forming units (PFU) of AdexICOSIg or AdexLacZ as a control was injected intravenously on day 0 or day 14 after immunization to study the preventive effects on EAM in the T cell activation phase and inflammatory phase, respectively. On day 21 after immunization, these animals were sacrificed, blood samples were collected from the heart, and the hearts were then removed, weighed, and divided for histological and biochemical examinations. Disease severity was estimated by the macroscopic and microscopic findings of the heart and heart weight to body weight ratios. In experiment 2, 5.0×10^9 PFU of AdexICOSIg or AdexLacZ as a control was injected intravenously (IV) on day 12 after immunization to study the preventive effects on severe EAM in the inflammatory phase. On day 19 after the first immunization, these animals were sacrificed, and disease severity was evaluated as described above. Macroscopic findings were classified into five grades as previously described²⁷⁾ with minor modifications: 0, no inflammation; 1, presence of a small discolored focus; 2, presence of diffuse discolored areas covering less than half of the cardiac surface; 3, diffuse discolored areas covering more than half but less than all of the cardiac surface; and 4, diffuse discolored areas covering all of the cardiac surface. Transverse sections of the heart specimens were prepared, fixed in phosphate-buffered 10% formalin, embedded in paraffin, and stained with hematoxylin and eosin. The areas of the entire heart and of regions affected by myocarditis were determined with the use of the NIH Image program (NIH, Bethesda, Maryland), and the area ratio (affected/total area in percent) was calculated.

Anti-cardiac myosin antibodies The 96-well plates were coated with purified porcine heart myosin (Sigma Chemical Co., St. Louis, MO, USA) at the concentration of 4 mg/well in 0.2 ml of PBS at 4°C overnight. Then 40 μ l of 50, 100, or 500-fold-diluted serum samples was applied to the myosin-coated plate and incubated for 1 hour at room temperature. After washing, 40 μ l of 100-fold-diluted alkaline phosphatase-conjugated anti-rat IgG1 or IgG2a (PharMingen) was added. After 1 hour, the plates were washed several times and the substrate for alkaline phosphatase (disodium-p-nitrophenyl phosphate-hexahydrate; 1 mg/ml) (Wako Pure Chemical Industries Ltd., Osaka, Japan) was applied to the wells. The absorbance at 405 nm was read and each sample was analyzed in duplicate. On day 21 after immunization as described in experiment 1, inguinal and popliteal lymph nodes were aseptically removed and lymph node cell suspensions were prepared by passage through a 200-gauge stainless steel mesh. Then cells were cultured in triplicate in 0.2 ml of RPMI 1640 medium supplemented with 10% fetal bovine serum, 1% non-essential amino acids (GIBCO BRL), and 5×10^{-5} M 2-mercaptoethanol at a cell concentration of 5×10^5 cells/well in 96-well flat-

bottomed micro titer plates. Cells were cultured with 50 pmol/ml of the purified porcine heart myosin (Sigma Chemical Co., St. Louis, MO, USA) in the presence of various concentrations of the anti-ICOS MAb and control antibody (mouse IgG1). The cultures were maintained for 72 hours at 37°C in humidified 5% CO₂ air. The wells were pulsed with 1 μ Ci/well of [³H] methyl thymidine for the final 18 hours of culture. Cells were harvested on glass fibers and incorporated [³H] thymidine was measured by a liquid-scintillation counting method.

We previously examined the expression of costimulatory molecules B7/CD28 and CD40/CD40L in EAM heart¹⁰. In this study we analyzed the expression of ICOS/ICOSL in the heart in both normal and EAM rats, using immunohistochemistry. ICOS was faintly expressed by myocytes in the heart tissue of normal rats, whereas ICOSL was mildly expressed on the endothelial cells. The expression of ICOS molecules was clearly induced on the infiltrating cells in EAM rats. Moreover, the expression of ICOSL on the infiltrating cells and endothelial cells in the heart was also enhanced in the EAM rat. To confirm that the ICOS/ICOSL pathway was involved in the development of EAM, we examined the expression of ICOS and ICOSL on lymph node cells and spleen cells by FACS analysis. ICOS expression was markedly enhanced on CD4, CD8, and CD25 positive cells in the lymph nodes of EAM rats as compared with normal ra, whereas, enhanced expression of ICOSL was detected in CD4-positive T cells, B cells, and macrophages (*M ϕ*) in the spleen of the EAM rat. Expression of ICOSIg was analyzed in the sera at different times after gene transfer, using ELISA. The maximum concentration was obtained 4 days after the administration of AdexICOSIg in the rats. The serum ICOSIg concentration decreased gradually, but was still maintained at around 1235 μ g/ml on day 7. However, the serum ICOSIg concentration was almost under the detection level at day 14. The effects of AdexICOSIg on EAM in experiment 1 is summarized in Table 1. The heart weight to body weight ratios, macroscopic scores, and % affected area ratios are shown in this table. No rats in the AdexLacZ-treated group spontaneously died during the 21 days of the experimental period. The heart weight to body weight ratios, macroscopic scores, and % affected area ratios were not significantly different between AdexLacZ-treated and AdexICOSIg-treated EAM rats when virus vectors were given at day 0. On the other hand, when the virus vectors were given at day 14, the heart weight to body weight ratios, macroscopic scores, and % affected area ratios were significantly improved in AdexICOSIg-treated EAM rats as compared with AdexLacZ-treated EAM rats. Rats treated with AdexLacZ developed severe myocardial lesions that were characterized by both enlargement and discoloration compared with the normal rat heart. The same degree of myocarditis was observed in the group treated with AdexICOSIg on day 0. On the other hand, minimal myocarditis was observed in the heart from the rat treated with AdexICOSIg on day 14. To examine the effects of AdexICOSIg on severe EAM, we next used high doses of the immunizing antigen to cause severe EAM in rats. Three of the twelve EAM rats

spontaneously died before treatment on day 12. All rats that died before day 12 showed macroscopic evidence of severe myocarditis and congestive heart failure at autopsy and thus were judged to have died of heart failure. We randomly separated the surviving rats into two groups that were treated with either AdexICOSIg or AdexLacZ. After AdexICOSIg treatment on day 12, no EAM rats died during the experimental period. Moreover, significant reduction in disease severity such as heart weight to body weight ratios, macroscopic scores, and % affected area ratios was achieved after AdexICOSIg treatment. Since the survival rate in the AdexLacZ-treated group was very low, both surviving and dead rats (within 1 hour from death) were subjected to further analysis. It should be noted that all EAM rats in the AdexLacZ-treated group had a large quantity of pericardial effusion, whereas no rat had any pericardial effusion after AdexICOSIg treatment. The AdexLacZ-treated EAM rats developed extremely severe myocardial lesions that were characterized by both enlargement and discoloration of the heart. More severe myocarditis was observed in the AdexLacZ-treated EAM rats. On the other hand, minimal myocarditis was observed in the hearts of rats treated with AdexICOSIg on day 12. All control rats treated with AdexLacZ developed typical severe autoimmune lesions in the heart that were composed of various inflammatory cells, including multinucleated giant cells, macrophages, and lymphocytes, and the loss of cardiac myocytes was also evident. The same degree of myocarditis was observed in the group treated with AdexICOSIg on day 0, although the multinucleated giant cells were less prominent. In sharp contrast, cardiac myocytes were well preserved with mild focal inflammatory cell infiltrates in the group treated with AdexICOSIg on day 14. Effects of AdexICOSIg treatment on day 14 on serum anti-myosin IgG1 and IgG2a antibodies were examined. On day 21 after immunization, sera were obtained from 6 rats per group. When antibody production was measured, AdexICOSIg administration was found to impede the production of anti-myosin antibodies of both the IgG2a and IgG1 isotypes. The IgG2a/IgG1 value in AdexLacZ-treated EAM rats was approximately 5, which indicated Th1 cytokine deviation, whereas the values in the AdexICOSIg treated rats on day 14 had a similar value, suggesting that delayed AdexICOSIg treatment did not change the balance between Th1 and Th2 cytokines. Lymph node cells obtained from the EAM rats had significant proliferative responses to cardiac myosin. Antigen-specific T cell proliferation was inhibited by the anti-ICOS antibody. The difference between the ICOS-antibody-treated group and control Ig-treated group was statistically significant. The inhibition of cell proliferation was achieved even when the anti-ICOS antibody concentration was reduced to 0.1 $\mu\text{g/ml}$. EAM has been used as a model for human myocarditis. Previous studies have shown that EAM in rats can be divided into two distinct stages²⁸). First, focal inflammation, mainly of macrophages, lasts up to day 14 after immunization. Subsequently, strong inflammation consisting of macrophages and CD4+T cells lasts up to day 19 after immunization and leads to myocardial cell destruction.

The activation and expansion of antigen-specific T cells occur during this inflammatory stage and these processes are regulated by the interaction of costimulatory molecules on T cells and APCs. The inflammatory stage features the production of Th1-type cytokines and pro-inflammatory cytokines, including IFN- γ , IL-1 β , and TNF- α ²⁸⁾. Second, degenerative and necrotic myocytes are replaced by fibrotic tissues and this recovery phase lasts up to days 25 to 36 after immunization. We previously demonstrated that B7/CD28 and CD40/CD40L molecules were expressed by the inflammatory cells and myocytes in pathologic foci of EAM, indicating that those two costimulatory pathways were involved in the induction of EAM. However, the abrogation of those costimulatory pathways by CTLA4Ig and/or CD40Ig could significantly inhibit the severity of EAM only when therapies were given before its manifestation, suggesting that another costimulatory pathway was critically involved in the progression of EAM. To search for the involvement of other costimulatory pathways and the means to treat ongoing EAM, we analyzed the expression of ICOS/ICOSL molecules on the lymph nodes, spleen, and heart in a rat model of EAM.

We found that the ICOS expression was enhanced on lymph node T cells and the ICOSL expression was augmented on the splenic CD4 T cells, B cells, and macrophages in EAM rats. These results were consistent with previous studies showing that the expression of ICOS was induced on T cells in the brain, and that the expression of ICOSL was induced on macrophages and B cells in the spleen in murine EAE (experimental autoimmune encephalomyelitis) models^{29), 30)}. Moreover, recent studies demonstrated the beneficial effects of an anti-ICOS antibody or ICOSIg on ongoing Th1 type autoimmune disease^{29), 30)}. Thus, it is conceivable that the ICOS/ICOSL pathway is critically involved in the process of EAM. Our approach was to use the *in vivo* production of the soluble form of ICOS, ICOSIg, by intravenous injection of an adenovirus vector containing it. Since human disease is diagnosed after the first clinical manifestations, it is critical to determine if a treatment is effective in ameliorating ongoing or established disease. For years, medical researchers have strived to develop selective immunotherapy's that could specifically ameliorate pathogenic immune responses without immunocompromising the patient. Blockade of many known receptors on T cells can inhibit the initiation of immune responses. However, this approach is problematic in the clinical setting since it is not possible to predict the onset of disease in patients³¹⁾. On the other hand, recent reports demonstrated that the pathway of ICOS/ICOSL, newly identified members of the B7 family, was critical for the effector phases of both Th1 and Th2 responses³²⁾, suggesting that blockade of this pathway might have therapeutic potential for the patient after the onset of disease. Actually, blockade of this pathway using an anti-ICOS antibody or ICOSIg has been reported to inhibit ongoing EAE^{29), 30)}. Thus, we analyzed the therapeutic effect of delayed treatment on EAM and found that the delayed blockade of ICOS/ICOSL had a marked, beneficial effect on ongoing EAM.

Unlike the blockade of B7/CD28 and CD40/CD40L pathways, the inflammatory responses and resulting myocardial injury were not significantly inhibited by AdexICOSIg treatment on day 0. It was shown that ICOS gene knockout or ICOS blockade during antigen priming resulted in the severe form of the disease in a murine EAE model. However, we could not detect any exacerbation of EAM by AdexICOSIg treatment. The discrepancy between previous reports and our finding has yet to be investigated, but might be explained as follows. First, it is possible that the anti-ICOS antibody transmits a signal to T cells that results in the subsequent T cell/APC interaction, whereas ICOSIg simply abrogates the interaction of ICOS/ICOSL. This hypothesis is supported by recent reports^{29), 30)}. A significant shift of T cell differentiation toward the Th1 type was achieved by the anti-ICOS antibody treatment, whereas the antigen priming of EAE-inducing T cells in the presence of ICOSIg *in vitro* resulted in the loss of the T cell ability to induce EAE. Another possibility is that the serum concentration of the antibody is highest at the time of injection, while in the case of AdexICOSIg, the highest concentration is achieved at around day 4. This time delay might cancel the deleterious effects of blockade of ICOS/ICOSL costimulation in the T cell activation phase.

The precise mechanism of the effectiveness of ICOSIg on ongoing Th1 type immune responses is unknown. However, there have been some hypotheses to explain it. An emerging concept is that ICOS costimulation may be more involved than CD28 costimulation in effector T cell responses³¹⁾. The effector phase of the immune response occurs after initial T cell activation and differentiation and involves the production of effector cytokines, and migration of differentiated T cells to the site of inflammation. Previous reports demonstrated that upregulation of the proinflammatory cytokine IFN- γ was suppressed in an intragraft by therapy with an anti-ICOS antibody in an allograft transplantation model³³⁾, suggesting that the production of effector cytokines was inhibited. In addition, blockade of ICOS costimulation during the efferent immune response in the EAE model results in the prevention of clinical disease associated with decreased splenocyte proliferation and IFN- γ expression, suggesting that the expansion of differentiated Th cells and the production of effector cytokines might be inhibited²⁹⁾. These results were consistent with our finding that blockade of the ICOS/ICOSL pathway could significantly inhibit antigen-specific T cell proliferation. Moreover, a recent study showed that ICOS costimulation played a critical role on the migration of CD4 positive memory T cells to the endothelial cells of the target organ³⁴⁾. In fact, we found the enhanced expression of ICOS and ICOSL on inflammatory cells and endothelial cells, respectively in the EAM heart. Furthermore, blockade of the ICOS/ICOSL pathway by AdexICOSIg resulted in inhibition of inflammatory cell infiltration into the heart.

In conclusion, we found that (1) ICOS and ICOSL are expressed by inflammatory cells and endothelial cells, respectively, in pathologic foci of EAM. (2) Blockade of the ICOS/ICOSL pathway by AdexICOSIg at the time of immunization

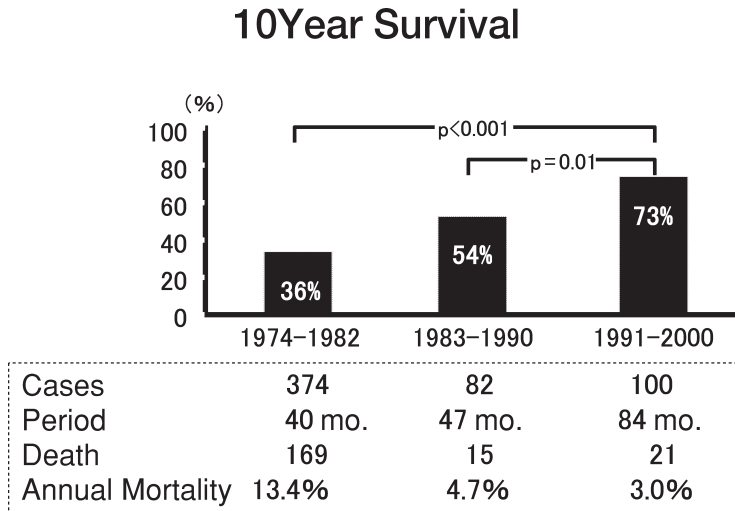


Figure 15 Changes in mortality in dilated cardiomyopathy (DCM) over the past 27 years, which divided three periods and to identify the factors that might have influenced survival.

neither inhibited nor exacerbated EAM. (3) In contrast, delayed treatment by AdexICOSIg could significantly ameliorate ongoing EAM (figure 15).

5. Clinical Application of Bench Work

Introduction

Dilated cardiomyopathy (DCM) is a primary disease of cardiac muscle characterized by decreased wall motion and ventricular enlargement. The variety of its causes and pathogenetic mechanisms may explain the heterogeneity of its clinical course. In addition to some patients who manifest heart failure in their younger age and rapidly deteriorate and those who die suddenly and unexpectedly, there are others who remain stable and asymptomatic for many years and who may improve. The overall prognosis is poor with a median survival of about two years after diagnosis, which was reported in 1981. Survival of patients with DCM may have been affected by earlier detection of the disease by the progress in echocardiography, referral bias and new therapeutic strategies such as pharmacological intervention. Thus, the clinical course of DCM through 20 century may have improved.

Objective:

To analyze the changes in mortality in dilated cardiomyopathy (DCM) over the past 27 years, which divided three periods and to identify the factors that might have influenced survival.

Materials and Methods

We have investigated changes in mortality associated with DCM during the past 30 years and to identify factors that might have influenced survival in our country. To analyze the changes in mortality in dilated cardiomyopathy (DCM) over the past 27 years, which divided three periods and to identify the factors that might have influenced survival. Three cohorts were enrolled to this study. In group III, after stratification for the severity of heart failure, patients were divided into 3 subgroups who were treated with both ACE inhibitors and beta blockers, treated with either ACE inhibitors or beta blockers, and treated with neither ACE inhibitors nor beta blockers.

Patients: 100 newly enrolled patients with DCM between 1991 and 2000 in our hospital and age was 53 ± 11.0 . After stratification for the severity of heart failure, patients were divided into 3 subgroups who were treated with both ACE inhibitors and beta blockers, treated with either ACE inhibitors or beta blockers, and treated with neither ACE inhibitors nor beta blockers. Figure 16 showed the Kaplan-Meier curves of the 3 cohorts. The upper line indicates patients treated with both an ACE inhibitor and a beta-blocker; the middle line indicates patients treated with either an ACE inhibitor or a beta-blocker; and the lower line indicates patients treated with

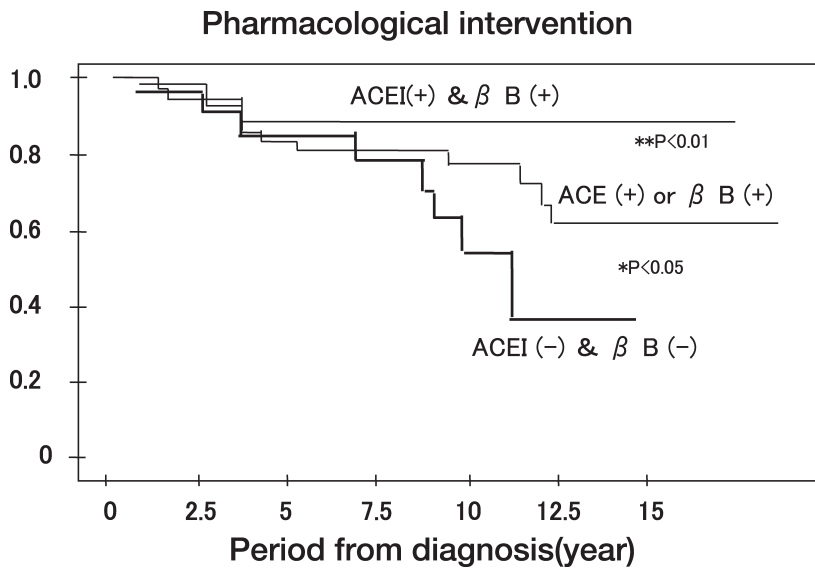


Figure 16 The effect of ACE inhibitor and beta-blocker on prognosis of DCM patients. ACEI: ACE inhibitors, β B: β blockers. After stratification for the severity of heart failure, patients were divided into 3 subgroups who were treated with both ACE inhibitors and beta blockers, treated with either ACE inhibitors or beta blockers, and treated with neither ACE inhibitors nor beta blockers. Figure shows the Kaplan-Meier curves of the 3 cohorts. Significant differences in mortality can be seen among the groups.

neither an ACE inhibitor nor a beta-blocker. Significant differences in mortality can be seen among the groups. Recent advances in pharmacological treatments, especially ACE inhibitors and beta blockers, have improved the prognosis of DCM. Discussion

Prognosis of DCM might be improved mainly by the advanced and widely spreaded diagnostic tools, such as echocardiogram, and also by progress in therapeutic strategies. DCM could be earlier diagnosed and its severity could become milder. It has been demonstrated by randomized clinical trials that ACE inhibitor, beta-blockers, class III anti-arrhythmic agents and AICD prolong life-expectancy. Although 80% or more of patients who applied for the heart transplantation were DCM in Japan, prognosis may be not necessarily bad. Furthermore, the variety of its causes and pathogenetic mechanisms could explain the heterogeneity of its clinical course. In the current study, prognosis of DCM has been improved over the past 27 years and significant differences in mortality can be seen among the treatment-groups. Recent advances in pharmacological interventions, especially ACE inhibitors and beta blockers, may have improved the prognosis of DCM. In addition to the earlier diagnosis, recent advances in pharmacological treatments, especially ACE inhibitors and beta blockers, have improved the prognosis of DCM.

Acknowledgments

The authors gratefully acknowledge Dr. Asano A. for providing cDNA for rat VEGF. We thank Drs. Xie Z. and Koyama T. for their technical assistance and critical comments. We thank to Toshiyuki Kudo, Hitoshi Sano, Keiji Yoneya, Masashi Watanabe, Hideki Kumamoto, Satoru Chiba, Yutaka Matsui, Nan Jia, Toshihiro Shimizu, Masatoshi Akino, Takahiro Tsukamoto, Takeshi Sugawara and especially to Drs. Kawaguchi H., Murakami M. Inobe M. and Uede T. for their critical contribution to the current study.

References

1. Braunwald E, et al. Heart Disease: A textbook of Cardiovascular Medicine. 6th edition Edited by E. Braunwald W. B. Saunders Company, Philadelphia, p546, 2002.
2. Kawaguchi H, Sano H, Iizuka K, et al. Phosphatidylinositol metabolism in hypertrophied rat heart *Circ Res* 1993; 72: 966-972
3. Kawaguchi H, Sano H, Okada H, et al. Increased calcium release from sarcoplasmic reticulum stimulated by inositoltriphosphate in spontaneously hypertensive rat heart cells. *Molecular and Cellular Biochemistry* 1993; 119: 51-57
4. Okamoto H, Kumamoto H, Chiba S, et al. Role of Microvasculature in Cardiac Remodeling Process. *Microcirculation Annual* 2001; 17: 36-38
5. Kumamoto H, Okamoto H, Watanabe M, et al. Long-term Effects of a New Ca²⁺ sensitizer, MCI-154, on Cardiac Function and Microvasculature in the Dilated Cardiomyopathic Hamster Heart. *Am J Physiol* 1999; 276: H1117-H1123

6. Yanagisawa-Miwa A, Uchida Y, Nakamura F, et al. Salvage of infarcted myocardium by angiogenic action of basic fibroblast growth factor. *Science* 1992; 257: 1401-1402
7. Okamoto H, Kawaguchi H, Sano H, et al. Microdynamics of the phospholipid bilayer in cardiomyopathic heart cell membrane. *J Moll Cell Cardiol*, 1994; 26: 211-218
8. Nakagawa I, Murakami M, Ijima K, et al. Persistent and secondary adenovirus-mediated hepatic gene expression using adenovirus vector containig CTLA4IgG. *Human Gene Therapy*. 1998; 9: 1739-1746
9. Ijima K, Murakami M, Okamoto H, et al. Successful Gene Therapy Via Intraarticular Injecion of Adenovirus Vector Containing CTLA4IgG in Murine Model of Type II CollagenInduced Arthritis. *Hum Gene Ther*. 2001; 12: 1063-1077
10. Matsui Y, Okamoto H, Kumamoto H, et al. Blockade of T cell costimulatory signals using adenovirus vectors could prevent both the onset and the progression of experimental autoimmune myocarditis. *J Molle Cell Cardiol* 2002; 34: 279-295
11. Kawaguchi H, Shoki M, Sano H, et al. PI response and calcium overload in cardiomyopathic hamster heart cell.
"New Aspects in the Treatment of Heart Failure" 1992; 36-40, Tokyo, Springer-Verlag.
12. Sano H, Okada H, Sakata Y, et al. Angiotensin II potentiates collagen synthesis in the hypertrophied heart "New Aspects in the Treatment of Heart Failure" 1992; 199-201, Tokyo, Springer-Verlag.
13. Shoki M, Kawaguchi H, Okamoto H, et al. Polyphosphoinositide metabolism in hypertrophic rat heart.
"New Aspects in the Treatment of Heart Failure" 1992; 202-204, Tokyo, Springer-Verlag.
14. Kudo T, Okamoto H, Mochizuki N, et al. Alteration in Cardiac renin-angiotensin system in spontaneously hypertensive rats (SHR) "New Aspects in the Treatment of Heart Failure" 1992; 234-237, Tokyo, Springer-Verlag.
15. Shoki M, Kawaguchi H, Okamoto H, et al. *Jap Circ J* 1992; 56: 142-147
16. Kawaguchi H, Shoki M, Sano H, et al. The studies of cell damaging and cell growth factors which induce cardiomyopathy. *Jap Circ J* 1992; 56: 1037-1044
17. Sano H, Okamoto H, Kitabatake A, et al. Increased mRNA expression of cardiac renin-angiotensin system and collagen synthesis in spontaneously hypertensive rats. *Molecular and Cellular Biochemistry* 1998; 178: 51-58
18. Onozuka, H. Fujii, S. Mikami, T. et al. In vivo echocardiographic detection of cardiovascular lesions in apolipoprotein E-knockout mice using a novel high-frequency high-speed echocardiography technique. *Circulation Journal* 2002; 66: 272-276
19. Shimizu, T. Okamoto, H. Chiba, S. et al. Long-term combined therapy with an angiotensin type receptor blocker and an angiotensin converting enzyme inhibitor prolongs survival in dilated cardiomyopathy. *Jpn Hert J* 2002; 43: 531-543
20. Shimizu T, Okamoto H, Chiba S, et al. Altered Microvasculature is Involved in Remodeling Process in cardiomyopathic Hamsters. *Jpn Heart J* 2003; 44: 111-126
21. Shimizu T, Okamoto H, Chiba S, et al. VEGF-mediated angiogenesis is impaired by angiotensin type 1 receptor blockade in cardiomyopathic hamster hearts. *Cardiovasc Res* 2003; 58: 203-212
22. Jia N, Okamoto H, Shimizu T, et al. A Newly Developed Angiotensin II Type 1 Receptor Antagonist, CS866, Regress Cardiac Hypertrophy Through Reduction in Beta-1 Integrin Expression. *Hypertens Res* 2003; 26: 737-742
23. Watanabe M, Kawaguchi H, Onozuka H, et al. Chronic effects of enalapril and amlodipine

- on cardiac remodeling in cardiomyopathic hamster hearts. *J Cardiovasc Pharmacol*, 1998; 32: 248-259
24. Sakamoto A., K Ono, M. Abe M, et al. Both hypertrophic and dilated cardiomyopathies are caused by mutation of the same gene, δ -sarcoglycan, in hamster: An animal model of disrupted dystrophin-associated glycoprotein complex. *Proc Natl Acad Sci USA*. 1997; 94: 13873-13878
 25. Murakami U, Uchida K, Hiratsuka T. Cardiac myosin from pig heart ventricle. Purification and enzymatic properties. *J Biochem (Tokyo)*. 1976; 80: 611-619
 26. Tamatani T, Tezuka K, Hanzawa-Higuchi N. AILIM/ICOS: a novel lymphocyte adhesion molecule. *Int Immunol*. 2000; 12: 51-55
 27. Okura Y, Takeda K, Honda S, et al. Recombinant murine interleukin-12 facilitates induction of cardiac myosin-specific type 1 helper T cells in rats. *Circ Res*. 1998; 82: 1035-1042
 28. Okura Y, Yamamoto T, Goto S, et al. Characterization of cytokine and iNOS mRNA expression in situ during the course of experimental autoimmune myocarditis in rats. *J Mol Cell Cardiol*. 1997; 29: 491-502
 29. Rottman JB, Smith T, Tonra JR, et al. The costimulatory molecule ICOS plays an important role in the immunopathogenesis of EAE. *Nat Immunol*. 2001; 2: 605-611
 30. Sporici RA, Beswick RL, von Allmen C, et al. ICOS ligand costimulation is required for T-cell encephalitogenicity. *Clin Immunol*. 2001; 100: 277-288
 31. Sperling AI. ICOS costimulation: is it the key to selective immunotherapy? *Clin Immunol*. 2001; 100: 261-262
 32. Sperling AI, Bluestone JA. ICOS costimulation: It's not just for TH2 cells anymore. *Nat Immunol*. 2001; 2: 573-574
 33. Ozkaynak E, Gao W, Shemmeri N, et al. Importance of ICOS-B7RP-1 costimulation in acute and chronic allograft rejection. *Nat Immunol*. 2001; 2: 591-596
 34. Khayyamian S, Hutloff A, Buchner K, et al. ICOS-ligand, expressed on human endothelial cells, costimulates Th1 and Th2 cytokine secretion by memory CD4+ T cells. *Proc Natl Acad Sci U S A*. 2002; 99: 6198-6203